MEASURE LOUDSPEAKER LOW-FREQUENCY RESPONSE, p. 12

June 2012
US $7.00/Canada $10.00

audioXPRESS

Advancing the Evolution of Audio Technology

Vacuum Tube Power Amps

Compact Driver Withstands the Test of Time

Speaker Frames and Structures

PLUS

- Achieve Higher Efficiency with Class B Amps
- An Interview with Ricardo Garcia, Founder of Base10 Labs
- An In-Depth Review of CES 2012
- New Products: A Multifunction Application Board and a Modular Audio Analyzer

www.audioXpress.com

From the Editor's Desk

The Demand for High-Quality Sound

It's an exciting time for *audioXpress* aficionados, as our magazine continues to evolve. We have already made a few strategic changes in content—adding new columns, providing more DIY projects, showcasing interesting interviews, and offering tutorials on audio engineering topics. Next month, we unveil the first stage of our redesign, beginning with a clean, bold font.

This month, we offer an issue filled with project potential. On page 12, Joseph D'Appolito teaches us how to make accurate loudspeaker frequency-response measurements with an anechoic chamber in his article, "Measuring Loudspeaker Low-Frequency Response."

On page 22, Dr. Gregory Charvat details the power amplifier design of his "Frankenstein" theater system. It's the second part of his series "Vacuum Tube Power Amps" article.

Didn't make it to the 2012 International Consumer Electronics (CES) Show? (CES) No worries. David J. Weinberg details many of the events and products he found at the show (p. 38).

In "The Science of Audio," Ricardo Garcia details his journey from his birth place in Medellin, Colombia, to his current home in Chicago, IL, and how he has found a way to meld his passion for music and love of science into a rewarding career.

Our columnists have also been busy testing various audio materials and equipment. On page 8, Mike Klasco and Steve Tatarunis explore the role adhesives play in sound quality. Richard Honeycutt explores power amp efficiency in "Hollow-State Class AB and B Amplifiers" in his article found on page 18. In the final column, Test Bench, Vance Dickason re-examines a driver he had previously used in "Another Look at Scan-Speak's 12MU/473100" (p. 29).

Regards,

C. J. Abate
editor@audioxpress.com

CONTENTS

VOLUME 43 NUMBER 6 JUNE 2012

Features

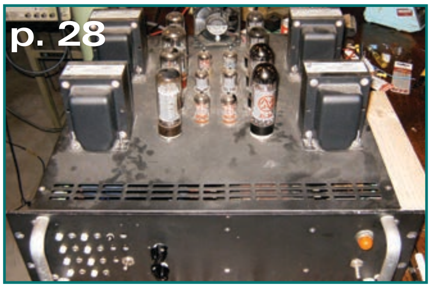

Columns

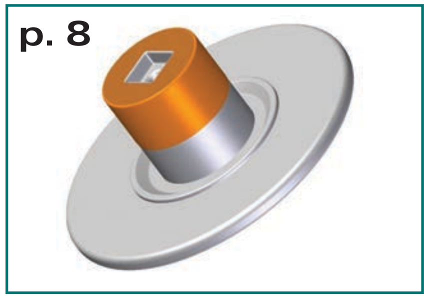

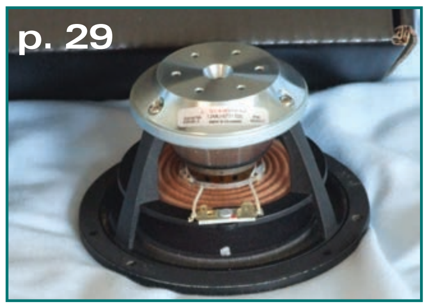

Departments

Websites

WEBSITES YOU SHOULD KNOW:
www.audioamateur.com
www.audioxpress.com
www.voicecoilmagazine.com
www.cc-webshop.com

Membership Counter

We now have 277285 members in 83 countries.

Not a member yet?

go to www.audioamateur.com

Supporting Companies

Not a supporting company yet?

Contact Peter Wostrel (peter@smmarketing.us), Phone 800.454.3741, 978.281.7708, Fax 978.281.7706 to reserve your own space for the next issue of our member magazine

Editorial Inquiries
Send editorial correspondence and manuscripts to:
audioXpress, Editorial Dept.
4 Park St., Vernon, CT 06066
E-mail: sbecker@audioXpress.com
No responsibility is assumed for unsolicited manuscripts. Include a self-addressed envelope with return postage. The staff will not answer technical queries by telephone.

Printed in the United States

SEGMENT LLC
audioXpress | VOICE COIL
WORLD TUBE DIRECTORY | LIS LOUDSPEAKER INDUSTRY SOURCEBOOK

 By Mike Klasco and Steve Tatarunis (United States)

Hard Parts

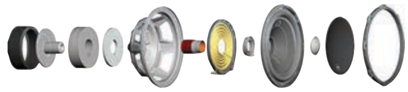

Magnetic Structures and Frames

An analysis of a speaker's hard structures

Speaker components can be separated into hard parts and soft parts. Until now, we have focused on the soft parts in this series. What move are the soft parts: the voice coil, cone, surround, spider, and dust cap. Hard parts include the magnet, the magnet steel return structure, and the frame to which all the speaker parts are assembled. This month, we'll check out frames and magnetic structures, but we will leave magnetic materials themselves for another month.

FRAMES

At first glance, the frame is the most low-tech part of the speaker, but actually, the frame defines the speaker. Another common term for the frame is the "basket," as all the parts are piled into this structure. Sometimes the tail wags the dog, as the stack-up—dimensions of the cone, spider, and voice coil—is determined by the speaker factory's existing frame inventory rather than optimum soft-parts selection engineering. The cone size, of course—as well as the depth of the cone, the way the spider attaches, and the cooling and cavity chamber issues—are all influenced by the basket.

The frame profile determines many speaker attributes. A deep frame enables a steep cone, which is likely for a subwoofer or woofer. A shallow frame tends to be used for a lower-excursion speaker or perhaps where mounting depth is a factor, such as autosound or in-wall or ceiling speakers. A large rear face enables a larger diameter spider and a larger-diameter magnetic structure, such as ferrite. A more compact frame rear face will limit the spider diameter, the voice coil diameter, and restrict use to neodymium magnetic structures.

The frame material has many implications. Frames can be stamped steel, cast aluminum alloy, or plastic. Each of these approaches can have an impact on distortion, power handling, and even sensitivity. Steel and plastic can reduce cost. Aluminum casting can impart an impression of style and quality. Steel frames tend to ring a bit, which is most apparent when they are not firmly mounted to a baffle. Carefully designed aluminum frames can help dissipate heat from the magnetic structure. Steel frames can drain a bit of flux from the top plate, thereby reducing speaker sensitivity (although stray flux interference with CRT TVs is not likely these days).

FABRICATION OF FRAMES

Steel frames are typically stamped from cold-rolled steel (see **Photo 1**). For deeper frames, progressive dies are used where the shape is formed step-by-step on multiple stamping tools.

Aluminum frames are often cast (see **Photo 2**). For short runs, aluminum frames can be sand cast, a manual operation that has a low tooling cost but a high unit cost. Aside from the time-consuming sand-casting process, extensive secondary finishing operations are needed. Once upon a time, labor was cheap in China and sand casting was popular. These days, this approach does not make sense for most products. One step up is gravity casting, and while the tooling cost is more expensive, the cost of parts is reasonable for medium quantities, and little machinery is needed. For large aluminum frame production runs, "investment tooling"—sometimes with multiple cavities (so more than one part is cast at a time)—is the way to go.

Plastic frames are often found on smaller- and mid-sized speakers (see **Photo 3**). For high production runs, the alignment of assembly of the rest of the speaker can be controlled by a plastic frame—either from the top plate being molded into the frame or the rear of the frame capturing the magnetic structure with special jigging. There can be thermal issues due to the lack of heat sinking, speed bumps have been known to crack optimistically design plastic frames with generous magnetic structures (such as heavy ferrite magnetic structures). Careful selection of engineering plastics and design are required for the designer to stay out of trouble.

The frame mounting flange that attaches to the enclosure baffle can be round,

Photo 1: A stamped cold-rolled steel frame (Source: Tanshi Electroacoustic Co. Ltd.)

Photo 2: A cast aluminum frame (Source: Ningbo Kingwin Machine Co., Ltd.)

Photo 3: A plastic frame (Source: Dongxin Electrical Machinery Co. Ltd.)

race track/elliptical, square-mounting tabs, or a pin cushion. Terminal tabs for the voice coil are mounted to the sides of the frame. The rear face of a frame can be bumped (in the tooling) to enable a flat spider to be used to avoid the nonlinearity of a bumped spider. Venting the frame behind the spider aides cooling and reduces the effects of power compression. Acoustic-resistance mesh is typically used to minimize debris. Frame attachments to the magnetic structure include swaging, screw mounting, welding, and even overmolding of the top plate in the case of plastic frames.

MAGNETIC STRUCTURES

Our series is not on the theoretical workings of speaker parts, but the physical implementations, and the fabrication process and attributes. Recent pricing trends are forcing a move away from compact, high-energy neodymium magnets back to ferrite. The physical topologies of the various magnetic structures have an impact on sound quality, including venting of air pressure and magnetic nonlinearity. Magnetic structure design also has an impact on sound quality, from design issues such as saturation of the top plate, aluminum bobbin eddy currents creating intermodulation distortion, and remedial techniques (e.g., copper cap on the pole piece, shorting rings, etc.).

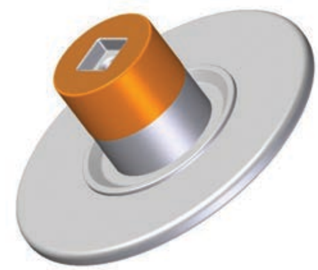

Photo 4: A cold-forged magnet part (Source: Million Interwork Sdn. Bhd.)

Forging is a manufacturing process involving the shaping of metal using localized compressive forces. Forging is often classified according to the temperature at which it is performed: either "cold" or "hot." Cold forging is the most common. A large (1,000-ton!) knuckle press bashes the steel part at room temperature, and the metal chunk oozes into the net shape. Forged parts, especially those that are hot forged, require further processing to achieve a finished part. As the steel is shaped during the forging process, its internal grain deforms to follow the general shape of the part. As a result, the grain is continuous throughout the part, giving rise to a piece with improved strength characteristics. Magnet steel, however, is low carbon for good magnetic circuit performance and is therefore soft (low carbon) steel. The top plate (washer) may lend itself to very low-carbon soft steel which is less prone to saturation (distortion), but it is hard to work with for back plates and pot structures (see **Photo 4**).

For most magnetic structures, the forming process is a type of precision forging. This process was developed to minimize cost and waste associated with post-forging operations. Therefore, the final product from precision forging needs little to no final machining, although tumbling in sand and other non-machining secondary processes are used. Using less material, and thus less scrap, decreasing the overall energy used, and reducing or eliminating machining helps reduce costs. Precision forging also requires less of a draft, which is fine for speaker-magnetic structures. Hot forging can provide superior performance in magnetic structures and is used in some higher-quality speakers. Hot forging requires some secondary machining operations. Powdered-metal forming has been used for speaker magnetic structures, but it is not common these days.

NEXT MONTH

Next month's column will cover neodymium, Alnico, ferrite, and even a bit on electromagnets and their associated magnetic structures. *aX*

MEMBER PROFILE

Member Name: Robert Nance Dee

Location: Catskill Mountains of NY

Education: State University of New York, military electronics and computer schools

Occupation: Semi-retired, writing, electronic engineering, patent prototyping

Member Status: Robert has subscribed to *audioXpress* off and on since the mid-1980s. He also has been a contributor for the past year or so.

Audio Interests: Robert is interested in analog tube and solid state pre-amplifiers, amplifiers, as well as turntable and tone arm design. He also focuses on digital interfacing, control of analog audio, and synchronous motor controls for turntables.

Most Recent Purchase: Dynaudio X12 speakers

Current Audio Projects: He is now working on an update of "Willow" (*audioXpress*, December 2011), a microcontrolled variable-frequency turntable motor controller, with a magnetic bearing turntable, and string-suspended arm.

Dream System: Robert's dream system consists of a Pass Labs XA30.5 power amp, an Ortofon MC A90 cartridge, Wilson Sophia speakers, and a Paradigm SUB15 subwoofer. A modified Merlyn pre-amp (see *audioXpress*, May 2012), turntable of his own design, arm, and motor system completes the package.

Robert Nance Dee

By Joseph D'Appolito (United States)

Measuring Loudspeaker Low-Frequency Response

Measure on-axis, far-field response free of room effects

With the availability of low-cost, PC-based acoustic data acquisition systems, experienced hobbyists can make highly accurate loudspeaker frequency-response measurements without an anechoic chamber. Popular systems include: CLIO, MLSSA, Praxis, and Sound Easy, to name a few. The power of these systems comes at a price. These systems window the time-domain measurement to eliminate room reflections. This, in turn, limits low-frequency response. Typically, response below 200 to 300 Hz is not possible in reasonably sized rooms.

The near-field technique—which was proposed by D. B. Keele, circa 1973—is the commonly accepted way to get low-frequency data without an anechoic chamber.[1, 2] However, there is another technique proposed by R. H. Small in an AES paper, circa 1971. His technique is simple. It does not require phase information and avoids some of the complexity of the Keele procedure, especially when there are multiple radiating surfaces. In this article, I'll review the Keele procedure and then present Small's approach. Examples of both are given and discussed.

THE PROBLEM

The goal is to measure the on-axis far-field response of a loudspeaker, free of any room effects. Reflected energy from the nearby floor, walls, and ceiling will arrive at the test microphone later than the direct wave. Depending on the path-length difference (therefore, the phase difference between the two arrivals) the reflected waves may add to or subtract from the direct wave.

Let's look at the effect of a single reflecting surface. Typically, if the speaker under test is placed on the middle of the floor, far from reflecting walls, the first reflection comes from the floor (see **Figure 1**). In this figure, the test driver and the test microphone are both at a 1-m height. The direct distance, d1, from driver to microphone is also 1 m. The wave reflected by the floor travels the longer path, 2d2 (see **Figure 1**).

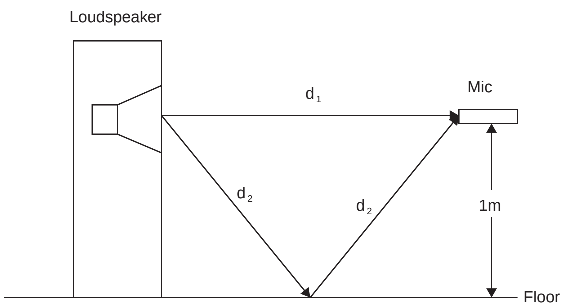

Figure 1: Floor reflection geometry

Whenever the distance 2d2 to d1 is equal to an even multiple of a wavelength, the direct and reflected waves will directly add. Whenever this distance is an odd number of half wavelengths, the reflected wave will be 180° out-of-phase and subtract from the direct wave. At intermediate distance-to-wavelength ratios, there will be partial addition or subtraction. The reflected wave will be somewhat weaker than the direct wave, since it travels a longer distance, so the direct wave will notcompletely cancel.

Figure 2 is a plot of the measured impulse response of a small two-way monitor loudspeaker. The MLSSA system was used for this measurement. Additional details on the measurement equipment are outlined at the end of this article. The measurement geometry is similar to that of **Figure 1**. Remember, the impulse response is the time-domain equivalent of frequency response. The two are related by the Fourier transform.

In this test, the direct on-axis wave arrives at the microphone about 2.8 ms after the test signal is applied to the loudspeaker. The floor reflection arrives at 6.3 ms and then there is 3.5 ms of reflection free data. If only the data between markers m1 and

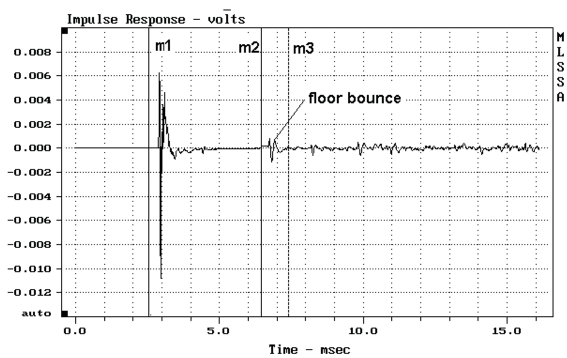

Figure 2: Measured impulse response of small two-way monitor

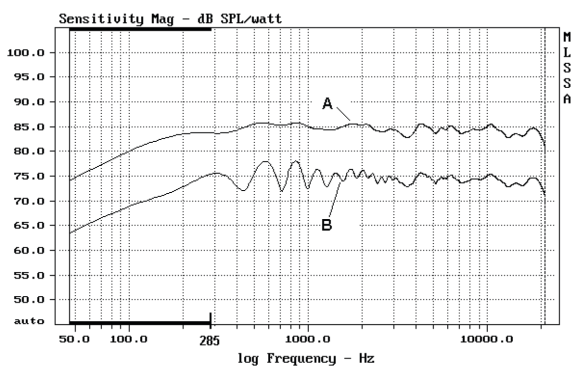

Figure 3: Response data: no bounce (A) with floor bounce (B).

m2 is analyzed, the relatively smooth frequency response is shown as curve A of **Figure 3**.

Extending the analysis up to marker m3 would now include the floor reflection and get the response shown in curve B of **Figure 3**. (The curves are offset by 10 dB for clarity.) Now you see the effect of the alternating addition and subtraction on the direct response caused by the reflected wave.

Because the full anechoic response is not achieved with the windowing process, this response is often termed "quasi-anechoic." And there is a catch! By using only 3.5 ms of data in this example, the lowest frequency resolved is:

$$f_{MIN} = \frac{1}{0.0035} = 285 \text{ Hz} \qquad [1]$$

This is shown by the black bars in **Figure 3** at the top and bottom of the plot. Any part of the curve plotted below that frequency is simply an artifact of the Fourier transform and does not represent valid data. Fortunately, there are ways to get the low-frequency data, which can then be spliced to the high-frequency data to get the full range response. I'll talk about them next.

ONE SOLUTION: THE NEAR-FIELD TECHNIQUE

In the near-field technique, the microphone is placed very close to the driver diaphragm to swamp out baffle and room effects. At low frequencies where the driver diaphragm behaves like a rigid piston, the measured near-field response is directly proportional to the far-field response and independent of the environment into which the driver radiates. Keele describes this technique in his paper.[1] I will summarize the approach and its limitations here.

For the near-field technique to work properly, the microphone should be placed as near to the center of the diaphragm as possible. Keele shows that a microphone distance less than 0.11 times the diaphragm effective radius results in measurement errors of less than 1 dB. As an example, a 6.5" driver will typically have an effective cone diameter of 5" or an effective radius of 2.5". For this driver, the microphone should be placed within 0.275" of the driver dust cap.

At higher frequencies, where cone break up begins, pressure waves from various areas of the diaphragm may arrive at the microphone out-of-phase, causing near-field response cancellations that are not observed at normal listening distances. For this reason, there is a practical upper limit to the near-field technique given in terms of driver diaphragm diameter. For a driver mounted in an infinite baffle, the limit is:

$$f_{MAX} = \frac{4,311}{D} \qquad [2]$$

Here f_{MAX} is in hertz and the driver diameter, D, is in inches. For closed-box or ported systems with finite baffles, this limit may be slightly lower. A 6.5"

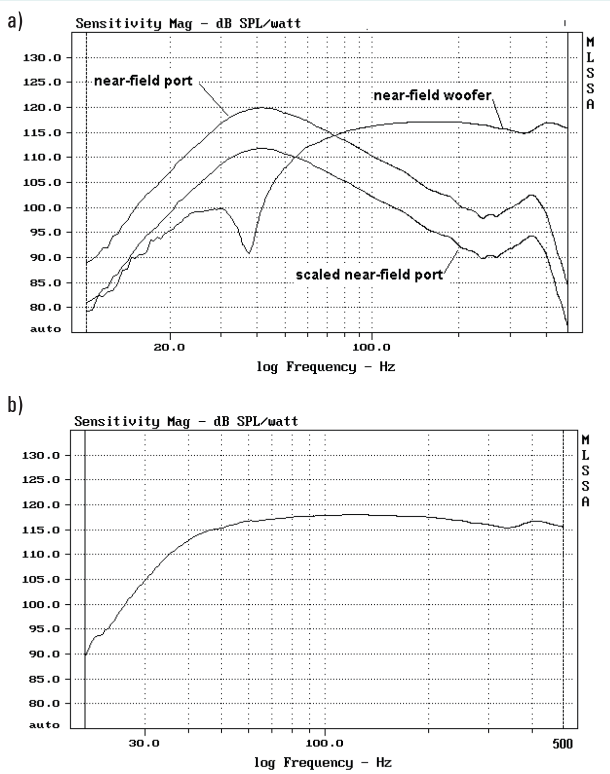

Figure 4a: Near-field woofer, port and scaled port responses; Figure b: Weighted sum of woofer and port near-field responses

driver example has:

$$f_{MAX} = \frac{4{,}311}{5} = 862\text{ Hz} \quad [3]$$

What happens when there are multiple radiating surfaces, as in a vented loudspeaker? Keele has the answer for that, too. He shows that individual near-field responses may be added with proper weighting to get the total near-field response. If all the radiating surfaces are circular, the addition looks like this:

$$P_{TOT} = D_1p_1 + D_2p_2 + D_3p_3 + \ldots + D_NP_N \quad [4]$$

P_{TOT} is the total near-field pressure. P_N is near-field pressure of the n^{th} circular radiating surface. D_N is the corresponding diameter of the n^{th} radiating surface. For example, if you are testing a vented loudspeaker with two woofers and two port tubes, you would take a total of four near-field measurements and add them together, after multiplying each one by its respective diameter.

If some of the radiating surfaces are rectangular, you can use the diameter of a circle with the same area. Alternatively, you can weigh all measured near-field pressures by the square root of the area, each respective radiating surface before adding them together.

The Keele approach seems pretty straightforward, but you must be careful of some things. First, Keele assumes all radiating surfaces are mounted on an infinite baffle. Under this condition, the radiation is into a "half-space" or a solid angle of 2π. However, most loudspeakers have relatively narrow baffles so they become omnidirectional at low frequencies. For this reason, the Keele approach may over estimate the low-frequency sound pressure level.

Second, the near-field pressures are complex quantities—that is, they have both magnitude and phase. If more than one radiating surface is involved in the testing, a simple pressure magnitude measurement is not enough. You need a system that measures both magnitude and phase to sum the responses correctly. Third, if radiating surfaces are close together, measurements may be contaminated by crosstalk. Finally, the upper-frequency limit on port pressure measurements tends to be much lower than a diaphragm of the same diameter. Even with these caveats, the technique is useful when there is no anechoic chamber.

It's time for an example. Consider the far-field on-axis response of the two-way monitor first examined in **Figure 2**. Let's look at the low-frequency response using the Keele approach. This speaker is vented so, both the woofer and port near-field responses must be measured. The results are plotted in **Figure 4a**. For the port measurement, the microphone was placed in the plane of the port exit.

At first glance, the port output seems to be 3 to 5 dB higher than the woofer output, which is a counter intuitive result. This is due to the diameter difference between the woofer and port. The port output can be scaled to the correct relative level by writing the summing equation in a different form:

$$p_{TOT} = p_{WOOFER} + \frac{D_{PORT}}{D_{WOOFER}}\, p_{PORT} \quad [5]$$

For this example, the woofer effective diameter is 14 cm and the port diameter is 5.5 cm, which gives:

$$\frac{D_{PORT}}{D_{WOOFER}} = \frac{5.5}{14} = 0.39 = -8.1\text{ dB} \quad [6]$$

The scaled version of the port response is also plotted in **Figure 4a**. Now you can see that it is more in line with the woofer level.

Before leaving **Figure 4a**, there are two interesting points not directly related to near-field testing. First, the sharp dip in woofer response at 37.6 Hz indicates the tuning frequency of the vented enclosure. In general, this value is more accurate than one obtained from the impedance curve, since it is not corrupted by voice coil inductance. Second, the up tick in port response around 340 Hz is caused by a standing wave associated with the internal height of the enclosure. When added to the woofer response, it produces a small dip in the total near-field response at the same frequency. However, this is not heard in practice because it is almost 15 dB lower than the woofer output and because the port exhausts to the rear of our two-way monitor example.

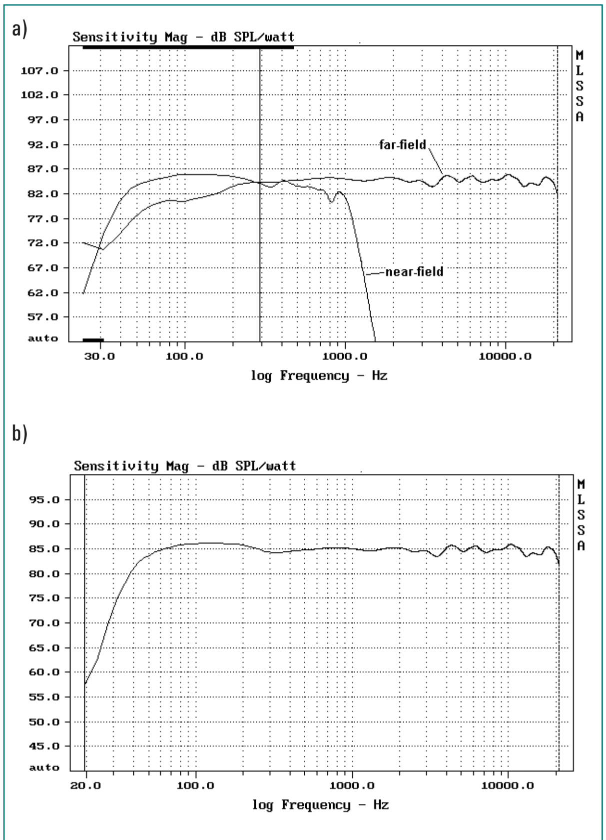

Figure 5a: Two-way monitor far-field and near-field responses; Figure b: Two-way monitor full range response

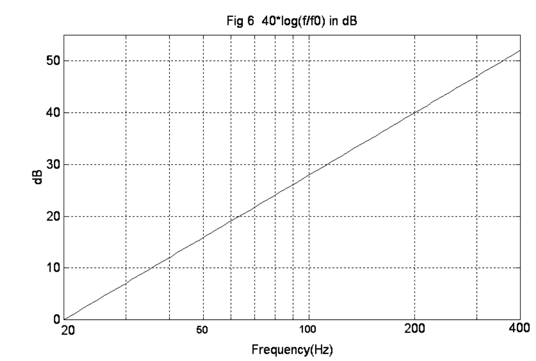

Figure 6: The 40*log(f/f0) in dB

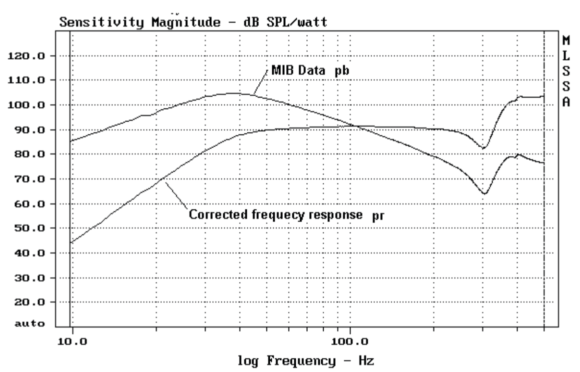

Figure 7: Two-way monitor MIB measurements

Adding the woofer and scaled port near-field responses provides the complete low-frequency response. This result is plotted in **Figure 4b**. At this point, the shape of the loudspeaker's low-end response is apparent. Now, splice it to the measured far-field on-axis response of our two-way monitor example.

The near-field data are valid below 780 Hz, but we have the small dip at 340 Hz. The far-field data are valid above 285 Hz. Clearly, the two graphs should be joined somewhere in the 285-to-340-Hz range. Regardless of the point chosen, the near-field response should always be brought into coincidence with the far-field response since the latter represents the true loudspeaker sensitivity.

In **Figure 5a**, I have shifted the near-field response level to meet the far-field curve just below 300 Hz. This point selection is somewhat arbitrary, but the result shown in **Figure 5b** looks reasonable. Notice that the response in the 70-to-200-Hz range is slightly elevated relative to the average far-field response. This may be a consequence of the "half-space" assumption in Keele's work. Absent an anechoic chamber, the near-field approach provides a good estimate of the low-frequency extension of the two-way monitor.

THE MICROPHONE-IN-BOX TECHNIQUE

Using the work of Benson, Small showed that, at low frequencies, there is a simple relationship between the sound-pressure level at a distance from an enclosure and the internal pressure within the enclosure, regardless of the number of radiating surfaces.[3, 4] This is an amazing result! To determine the low-frequency response of the two-way example, only one measurement of pressure inside the enclosure is needed! Not only that, but because there is only one measurement, phase information is not required. The governing equation can be written as follows:

$$p_R = kf^2 p_B \qquad [7]$$

p_R is the pressure at a distance outside the enclosure. p_B is the pressure inside the enclosure. k is a constant. f is the frequency in hertz.

Equation 7 is not too useful in its present form. The squaring operation will lead to rather large numbers. This can be avoided by normalizing the equation to the starting frequency, f_0. Furthermore, the result should be in decibels. So, first rewrite **Equation 7** like this:

$$p_R = k\left(\frac{f}{f_0}\right)^2 p_B \qquad [8]$$

k is now a different constant. Now, take the logarithm of both sides and multiply by 20 to convert **Equation 8** into an equation in decibels:

$$20\log(P_R) = 20\log(k) + 40\log\left(\frac{f}{f_0}\right) + 20\log(p_B) \qquad [9]$$

or:

$$p_R\ (\mathrm{dB}) \propto 40\log\left(\frac{f}{f_0}\right) + p_B\ (\mathrm{dB}) \qquad [10]$$

The symbol "∝" can be read as "proportional to." Recall that the logarithm of a squared quantity is just twice the logarithm of the quantity itself. Now, the large number squaring has been avoided. Ignore the term "20 log(k)" since it just adds to the level but does not change the shape of the curve. To make things even easier, I plotted the following term:

$$40\log\left(\frac{f}{f_0}\right)$$

It is in decibels in **Figure 6** for a starting frequency, f_0, of 20 Hz.

Now, the process is very simple. All you need is an AC voltmeter with a decibel scale, an audio oscillator, a good microphone, and an amplifier. Start at 20 Hz. Increase frequency in 10-Hz steps. Read the internal pressure in decibels off the AC voltmeter. Add the appropriate correction using the plot in **Figure 6**. Repeat these steps until reaching 400 Hz, and plot the results. I have dubbed this process the "Microphone-in-Box" technique, or MIB. P_R is the pressure-response shape. Scaling it to the far-field response is still necessary.

As with the near-field approach, there are some caveats to consider when using the MIB technique. First, there is the same half-space assumption as in the near-field approach. Second, it is assumed that the pressure p_B within the enclosure is uniform. Once standing waves build up, the equation breaks down. Small thought the data would be good up to a frequency where the largest dimension of the enclosure equals 0.125 of a wavelength. My experience indicates that this assumption is somewhat pessimistic. In practice, it is fairly obvious from the data where the technique breaks down. There are also some effects at higher frequencies due to enclosure losses that I will not discuss here.

Let's take a second look at our two-way monitor with the MIB technique. I have programmed my MLSSA system to take the in-box measurement and automatically apply the correction curve of **Figure 6**. I passed a microphone through the port tube and placed it close to the geometric center of the enclosure. **Figure 7** shows the in-box pressure measurement taken at that location. The in-box pressure response peaks close to the box tuning frequency of 37.6 Hz. Above and below that frequency in-box pressure response falls off by 12 dB/octave. After applying the correction, you get the low-frequency response also shown in **Figure 7**. It is clear in this example that the MIB technique breaks down somewhere above 250 Hz due to the standing wave within the enclosure.

It is interesting to compare the two low-frequency response methods. This comparison is plotted in **Figure 8**. Agreement is quite good between 50 and 200 Hz. However, below 60 Hz, the near-field result rolls off more quickly than the MIB result. I tend to believe the MIB result below 50 Hz. There are two reasons for this. First, below f_B, the woofer and port are out-of-phase, so the response in that range results from a subtraction of two relatively large quantities to get a small difference. A small error in the effective diameters of either the port or woofer, or both, will lead to a response error here. Second, the near-field signal-to-noise ratio (SNR) is poor at very low frequencies, requiring several averages of the data to get a reliable result.

This point is illustrated in **Figure 9**. Here the woofer near-field data is plotted after four averages. The MIB in-box pressure is not averaged at all. The input signal level is the same for both plots. The difference is obvious. I used 16 averages to get the near-field results shown in this article. Of course, you can increase the test-signal level to get a better SNR, but you must be careful. If the port velocity gets too high, the port response becomes nonlinear and the results are invalid.

As a final example, let's look at results from the testing of a sealed-box subwoofer with two 12" drivers. These tests were run to get the unequalized subwoofer response. The data was then used to design an electronic equalizer for

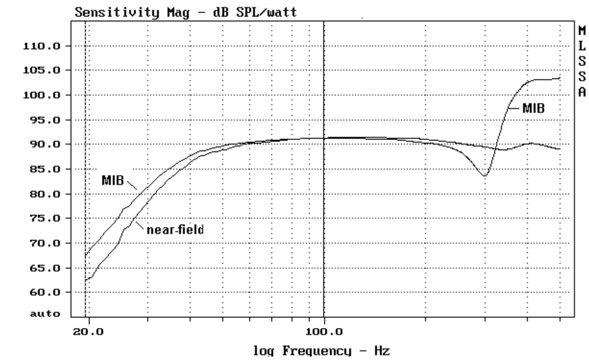

Figure 8: Comparing near-field and MIB responses

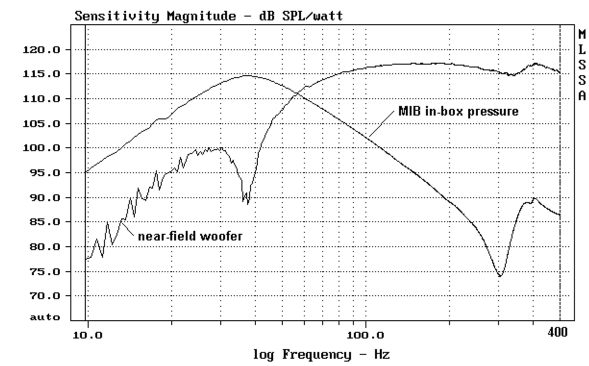

Figure 9: An illustration of the signal-to-noise issue

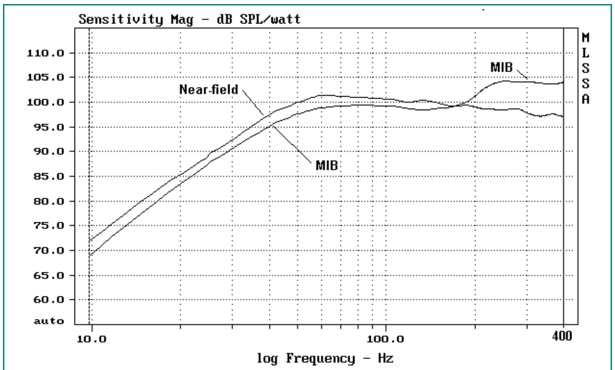

Figure 10: Example of a subwoofer

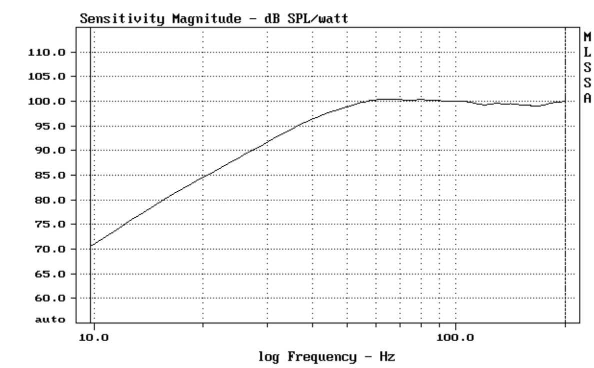

Figure 11: Average of near-field and MIB subwoofer responses

the subwoofer.

Near-field and MIB data are plotted in **Figure 10**. Near-field measurements of both woofers were taken and added together. The woofers are mounted on opposite sides of the enclosure so there was little chance of cross-contamination. The near-field magnitude responses of the two woofers were identical and could be added together without regard to phase. Fortunately, in this example, there was no port response to consider. A 0.75" hole had to be drilled in the test box to insert the microphone for the MIB test. The space around the microphone cable was sealed with Blue Tac.

Looking first at the near-field result, it is relatively smooth from 10 Hz all the way out to 400 Hz. There is a gentle rise of about 1 dB in response centered around 60 Hz. The MIB response is flat in this region, but breaks down above 200 Hz. Both responses show the expected 12 dB/octave roll off below 40 Hz.

Which one is right? It is difficult to know. But remember, both techniques just give us the response shape. We can change the relative level. If we set the two responses equal at 100 Hz, the curves then differ by no more than 1 dB anywhere from 10 Hz to 160 Hz. For design purposes, I averaged the two responses. The result is shown in **Figure 11**. For subwoofer equalizer design, data up to 200 Hz was sufficient.

RELIABLE ESTIMATES

Both techniques described in this article produce reliable estimates of loudspeaker low-frequency response in the absence of an anechoic chamber. Both techniques agree reasonably well given their different approaches to the problem.

On the plus side, the near-field approach tends to be valid over a wider frequency range. But, except for the single-woofer case or the sealed-box subwoofer example, phase information is required to properly add the individual radiating surface responses. Also, response error below a vented speaker's tuning frequency is possible. Increasing the drive level for better SNR can help in this case.

The big advantage of the MIB technique is that it requires only a single measurement of in-box pressure to get speaker response, regardless of the number of radiating surfaces. As a result, phase data is not needed and manual point-by-point measurements may be used.

Generally, the valid frequency range for the MIB measurement is smaller than that of the near-field approach. The microphone should be placed near the geometric center of the enclosure away from walls and interior baffles. With seal-box systems, getting the microphone into the enclosure may present a problem. *aX*

Author's note: The test equipment listed below was used to develop the data presented in this article.

SOURCES

MLSSA 10.3 acoustic data acquisition card
DRA Laboratories | www.mlssa.com

B&K 4191 0.5" Laboratory-grade condenser microphone, **B&K Type 2669 Pre-amp microphone pre-amp**, and **B & K Microphone calibrator**
Brüel & Kjær | www.bksv.com

Listen Sound Connect microphone power supply and amplifier
Listen, Inc. | www.listeninc.com

CLIO Model 2 Power amp for speaker testing
Audiomatica | www.audiomatica.com

REFERENCES

[1] D. B. Keele, "Low-Frequency Loudspeaker Assessment by Near-Field Sound Pressure Measurement," *Journal of the Audio Engineering Society*, 1974.

[2] J. A. D'Appolito, *Testing Loudspeakers*, Audio Amateur Press, 1998.

[3] J. E. Benson, "Theory and Design of Loudspeaker Enclosures," IREE (Australia), 1969.

[4] R. H. Small, "Simplified Loudspeaker Measurements at low Frequencies," *Journal of the Audio Engineering Society*, 1972.

 By Richard Honeycutt (United States)

Hollow-State Class AB and Class B Amplifiers

Achieving higher efficiency with Class B amplifiers

Last month, I pointed out the importance of efficiency in power amplifiers, and that Class A amplifiers are limited to a maximum possible efficiency of 25%. Class B amplifiers, in which the tubes are biased at cutoff, can operate at much higher efficiencies.

CLASS B OPERATION

If an amplifier tube is biased at cutoff—so that the tube only conducts on one half-cycle of each signal cycle—you can achieve more than 70% efficiency. Of course, this means in order for the output signal to be a reasonably accurate replica of the input signal, two output tubes must be used: one for the positive half-cycle, and one for the negative half-cycle. Using this approach, a pair of 6550 beam power tubes (rated at 35-W plate dissipation each) can theoretically produce 160 W of output power. In practical circuits, two 6550s usually provide about 100 W of output.

TRANSFORMER-COUPLED PUSH-PULL

Figure 1 shows a simple Class B push-pull power amplifier circuit. To make one of the two tubes provide positive half-cycles of the output, you can use a phase splitter or inverter at the input and output. This is true because with the output tubes biased at cutoff, only a positive signal at the grid will produce an output at the plate. Since the signal at the plate is out of phase with the grid signal, a Class B biased tube can only produce negative half-cycles at the plate. In the circuit shown, I used a driver transformer to reverse the phase at the input to one tube. The output transformer reverses the phase from the output of that tube. This action is shown by the signal-voltage waveforms in **Figure 1**. This circuit uses a negative voltage supply (C–) for fixed biasing of the grids.

PHASE SPLITTERS – PARAPHASE

Although driver transformers have been used in many power amplifiers, they are expensive and heavy. They can also provide challenges in terms of frequency response and distortion performance. Therefore, several types of phase splitters using tubes have been invented. The earliest is most likely the "paraphase" circuit shown in **Figure 2**.

This is just a two-stage amplifier, with the first stage feeding the upper output tube grid and the second stage feeding the lower output tube grid. In order to provide opposite phases, the grid of the phase splitter's second stage is fed from the output of the first stage through a voltage divider. The voltage divider reduces the signal voltage to the second-stage grid, so it has the same amplitude as the signal voltage at the first-stage grid, and the output waveforms at both plates will have equal amplitudes. In order to provide a symmetrical, low-distortion output from the push-pull power tube stage, the resistor values need to be closely matched, as do the halves of the 12AU7 dual triode (usually true for dual triodes). Even so, unless negative feedback is used, this circuit does provide some asymmetrical distortion. The application of negative feedback will be discussed later.

DIFFERENTIAL AMPLIFIER (LONG-TAILED PAIR)

If the cathodes of two triodes or pentodes are fed through a single large resistor, they are forced to share an essentially constant current. The way this works is that an input signal feeds the grid of the left-hand triode, while the right-hand triode's grid is grounded. A positive grid voltage on the left-hand triode causes an increase in plate current in that triode. This current is also the cathode current,

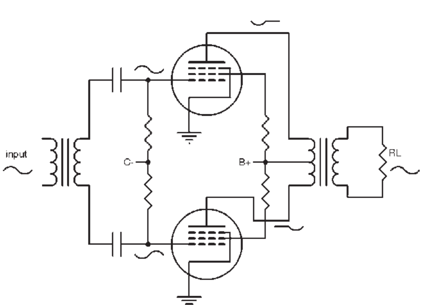

Figure 1: A simple Class B push-pull circuit

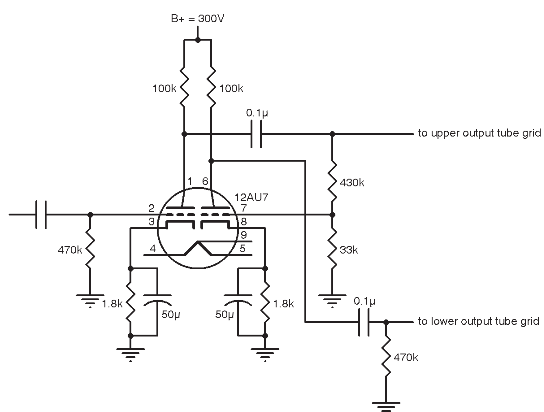

Figure 2: A paraphase phase splitter

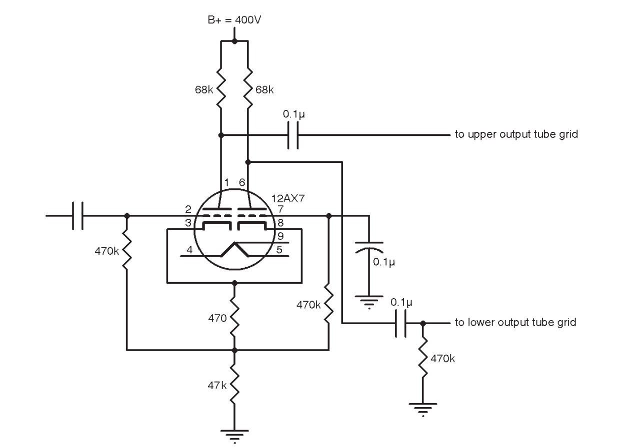

Figure 3: A differential amplifier phase splitter

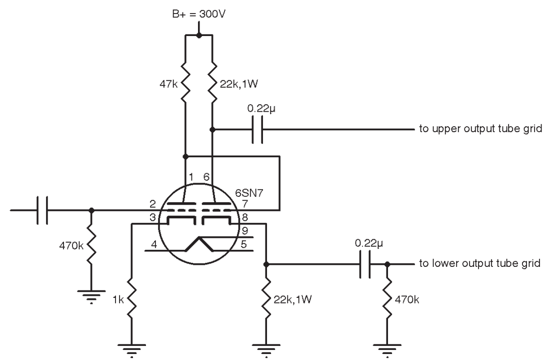

Figure 4: A split-load phase inverter

and when it increases, it raises the cathode voltage of the tube. Since the cathodes are connected, when the cathode voltage of the left-hand triode increases, so does the cathode voltage of the right-hand triode, decreasing the grid-to-cathode voltage of the right-hand triode and reducing its plate current. Since the output at either plate is proportional to the difference between the two grid voltages, the circuit is called a "differential amplifier," or sometimes a "long-tailed pair" (see **Figure 3**).

This circuit tends to produce much less distortion than the paraphase circuit, especially if the plate resistors are well-matched.

SINGLE TRIODE OR SPLIT-LOAD PHASE INVERTER

Perhaps the simplest-looking phase splitter uses a single triode providing outputs at both the plate and the cathode. The trick is that, in order to make this idea work, you must use equal plate and cathode resistors, which in turn requires the grid to be biased at a high positive voltage—about half of B+. This is usually accomplished by the use of a pre-driver stage whose plate is direct-coupled to the grid of the phase splitter. The circuit incorporating both the pre-driver and the phase splitter is shown in **Figure 4**.

This circuit was used in the well-known amplifier circuit introduced by D. T. N. Williamson in 1947. It is an inherently low-distortion phase splitter, but

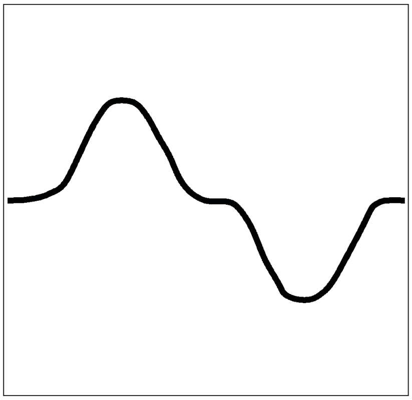

Figure 5: Crossover distortion

as with the previous two, the plate and cathode resistors should be wellmatched.

BIASING AND THE AB CLASSES

True Class B amplifiers have been spurned by critical listeners because they generate an especially annoying form of distortion called "crossover distortion." This distortion results from the fact that any tube's performance is nonlinear when operating near cutoff. The waveform resulting from crossover distortion is shown in **Figure 5**.

The reason crossover distortion is so annoying is that, whereas other forms of distortion are generally proportional to the output voltage—meaning they become objectionable only when the amplifier is seriously overdriven—crossover distortion components have an essentially constant level regardless of the output voltage. Thus, at low signal levels, the distortion percentage can be quite high. The result is a granular, gritty sound.

The unpleasant effects of crossover distortion can be mitigated if both output tubes are biased slightly or when there is no signal. Then the nonlinear operation in one output tube occurs when the other tube is conducting heavily and producing a robust output, so that the audibility of the distortion components is reduced. This type of biasing is identified as "Class AB." Depending upon the amount of quiescent current, it may be Class AB_1 or Class AB_2. Most audio circuits use Class AB_1. In Class AB_2, the grid is biased slightly less negative than in Class AB_1, making it draw grid current on positive signal peaks. This, of course, produces more distortion but produces slightly more output power.

Setting the bias on a push-pull amplifier usually involves adjusting the voltage of the grid-bias (C–) supply while applying a signal to the power amplifier and monitoring the output wave on an oscilloscope. At the ideal bias, crossover distortion will disappear from the waveform. This should be done carefully, since if the bias is insufficiently negative, the tubes may draw too much quiescent current, shortening their life, and/or perhaps blowing fuses.

FEEDBACK

In an earlier article, I discussed an important 1927 invention by H. S. Black of Bell Telephone Laboratories: negative feedback (patented 1937). This idea involves applying a fraction of the output signal of an amplifier with inverted phase to the input. The feedback signal can be proportional to either the voltage or the current of the output.

Negative feedback has several important effects. It flattens frequency response, reduces distortion, modifies the amplifier's input and output impedances, and makes amplifier performance less dependent on the characteristics of particular vacuum tubes. Negative feedback can be applied to a single stage, or globally to the entire amplifier. **Figure 6** shows two forms in which single-stage negative feedback can be applied.

The voltage feedback circuit applies part of the plate signal to the grid through a feedback resistor—in this case, 10 MΩ. The current feedback circuit uses an unbypassed cathode resistor to create the feedback signal at the cathode, as discussed in a previous article.

As with most things, however, negative feedback does not provide a free lunch. The use of negative feedback always results in reduced gain. The effect of flattening frequency response is related to the decrease in gain. Any amplifier has a "gain-bandwidth product" (GBW) that is essentially constant, regardless of the presence or amount of negative feedback. Thus, a voltage amplifier with a gain of 20 and a frequency response that is flat up to 200 kHz will have a GBW of 4 MHz (i.e., 20 × 200 kHz). If the gain is reduced to 10 by use of negative feedback, the GBW remains the same at 4 MHz, but the frequency response will now extend to 400 kHz. Note that the GBW is still 4 MHz (i.e., 10 × 400 kHz). Voltage feedback reduces an amplifier's effective output impedance. Current feedback increases it.

Figure 7 shows the limitations of the distortion reduction provided by negative feedback. Note that although negative feedback reduces the distortion at most output levels, it does not and cannot increase the maximum output voltage defined by the onset of hard clipping, which is determined by the B+ voltage, load resistance, and component values in the circuit. What actually happens is that, rather than exhibiting a gradual increase in distortion as the output voltage increases, the circuit with negative feedback exhibits low distortion until hard clipping is reached, then the output suddenly becomes essentially a square wave.

The aural effect of small amounts of harmonic distortion is a change in the timbre of the instrument or voice. Particularly in vacuum tube circuits, where

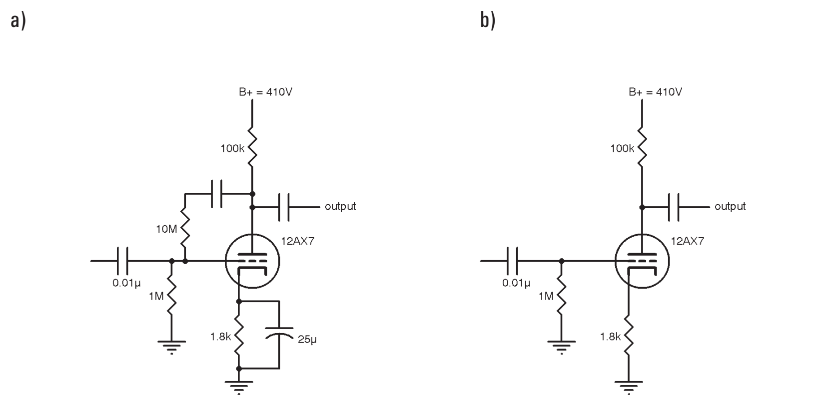

Figure 6: Single-stage negative feedback: voltage feedback (a); current feedback (b)

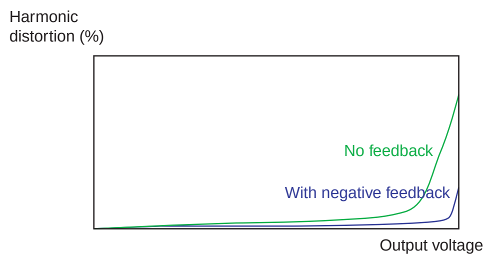

Figure 7: The effect of negative feedback on distortion

the predominant harmonics are low-order (second and third), the effect is relatively innocuous. But, when hard clipping begins, the relative content of higher-order harmonics (as high as 10th and above) increases. These harmonics are aurally obnoxious to most people, although they are deliberately introduced as special effects in some forms of music. Thus, whether or not negative feedback is beneficial for audio amplifiers has been a subject of debate. The answer probably depends upon the extent of overdriving the amplifier encounters in normal use. A much more thorough discussion of the aural effects of distortion will be presented in a future article.

Feedback can also be applied "globally," around a complete multistage amplifier. In 1947, Williamson published a circuit for a power amplifier using global feedback. In order to provide low distortion and maximum stability against parasitic oscillation (the amplifier behaving as an oscillator), he used a split-load phase inverter. The global feedback loop included the output transformer in order to reduce the effects of transformer-introduced distortion. The Williamson circuit became a de-facto standard design for tube audio power amplifiers in the 1950s and 1960s.

Another method of applying global feedback is the "ultra-linear" circuit invented by Alan Blumlein. This circuit incorporates a tap on the output transformer primary, from which negative feedback is applied to the screen grids of the output tubes. This approach has been described as a way to obtain the lower distortion of a triode along with the higher output power of a pentode or beam-power tube.

COMPLETE PUSH-PULL POWER AMPLIFIER

Figure 8 is a schematic diagram of a commercial 15-W power amplifier. For clarity, the power supply components are omitted. Tube V1, the left-hand unit of the 12AX7 dual triode, serves as a pre-driver. The 100-pF capacitor in parallel with the plate resistor of V1 helps to stabilize the amplifier against parasitic oscillation. V1 is direct-coupled to the grid of V2, which is the split-load phase inverter. For lowest distortion, the 150-kΩ plate and cathode resistors should be matched in value.

The output tubes are 6L6GC fixed-bias beam-power tubes. The –50-V bias supply is normally adjustable via a potentiometer so the crossover distortion can be minimized by biasing the tubes at their optimum Class AB$_1$ operating point. If the output tubes are matched, the distortion is minimized. Most output tubes are available in matched pairs.

The screen grids are usually fed from a power resistor (in this case, about 250 Ω, 5 W—not shown) connected between the screen grids and the B+ supply (identified as "405 V" in this circuit). The screen grids are decoupled by an electrolytic capacitor, probably about 40 µF (also not shown), connected from the screen grids to ground. The control grids of the output tubes are fed through 1-kΩ resistors to prevent parasitic oscillation.

Global feedback is provided via a 75-kΩ resistor connected to the output transformer secondary and feeding the cathode of V1. This signal is out of phase with the signal at V1's control grid, reducing the AC grid-to-cathode voltage and thus providing negative feedback. A 100-pF capacitor parallels the 75-kΩ resistor, enhancing stability against parasitic oscillations.

In future articles, I will look at some more specialized vacuum tube circuits. But next month, I will lighten up a bit. I'll present an interview with Kevin Shaw of Shaw Audio, a Nashville-area boutique musical instrument amplifier company. *aX*

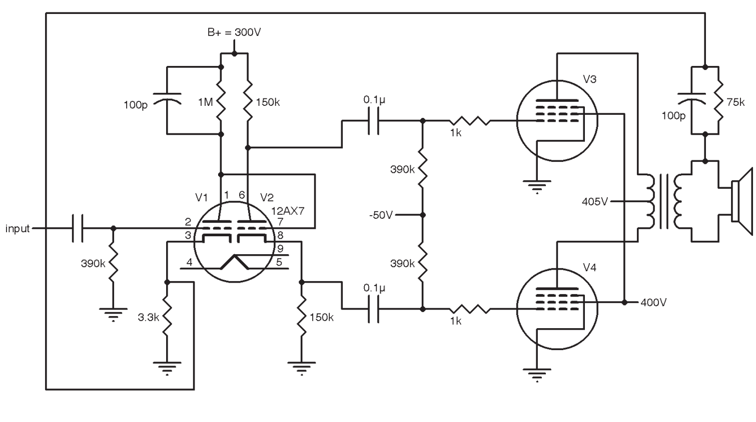

Figure 8: A complete push-pull amplifier

By Dr. Gregory L. Charvat (United States)

Vacuum Tube Home Theater System (Part 2)

Vacuum Tube Power Amps

Details about vacuum tube power amps in the "Frankenstein" system

Initially developed in college during my undergraduate years, the home theater system earned the name "Frankenstein," because it was the largest audio system in the dormitory (see **Photo 1**). It is a 7' tall vacuum tube home theater system mounted into a military surplus equipment rack from World War II that is enameled in black crinkle paint and topped with an menacing back-lit sign that reads "DANGER POWER ON."

Developing a vacuum tube home theater system is expensive because modern movie tracks are six channels (front R/L, rear R/L, front center, and subwoofer) requiring six power amplifiers. Power levels must be sufficiently high so clipping does not occur during loud explosions in war movies or other action sequences. *audioXpress* readers may agree that powerful tube-audio amplifiers are not inexpensive.

In the first portion of this series, I covered the system's architecture and circuit-level details. Now, I'll detail the power amplifier designs that provide relatively high-peak power for movies.

PHILOSOPHY

Fortunately, action movie sound tracks are generally quiet during dialog and plot development, with the occasional loud action-filled scenes. Vacuum tube power amplifiers are ideally suited for these scenes.

Tubes are capable of handling significantly more instantaneous power than their rated average power. This is the reason why tubes are used in radar systems requiring high-peak power supporting low-duty cycle pulses.[1] In radar systems, this peak power can reach several orders of magnitude greater than the average power rating for the tube.

A tube-power amplifier was developed using the radar design philosophy. The RMS power capability of this amplifier exceeds the specification for the output tubes because the amplifier is meant to run at maximum power for only short periods of time, leaving the higher RMS power available for loud action scenes.

This design pushes EL34s to the limit, providing 80-W RMS per channel for the front and rear speakers and 52-W RMS for the subwoofer in a mode somewhere between Class AB and B. EL34s in Class AB mode are capable of providing 40-W RMS of power. Therefore, this design can only supply its maximum power for a finite amount of time before overheating occurs.

SYSTEM BLOCK DIAGRAM

The Frankenstein supports two modes: high-fidelity stereo and home theater. The analog outputs from a surround-sound processor and a McIntosh C-24 high-fidelity stereo preamplifier are fed into an audio switch matrix inside the audio transfer switch and surround pre-amplifier. In high-fidelity mode, the C-24's output is routed to the power amplifiers. In surround-sound mode the output from the surround processor is routed to the power amplifiers. Refer to the first article in this series for details as well as a block diagram and call-out diagram.[2]

There are five power amplifiers, audio input to each is sourced from the audio transfer switch and sur-

Photo 1: The Frankenstein, a vacuum tube home theater system

plifiers are built into the quad-power amplifier, driving the front and rear speakers. The mono-block power amplifier drives the subwoofer. There is no center-channel amplifier, but the connections are builtin to add one.

The amplifier architecture is a negative feedback, high-fidelity amplifier include a differential amplifier, a loop compensator, a phase splitter, and a push/pull output (see **Figure 1**).

THE MONO BLOCK POWER AMP

The mono block power amplifier's power supply provides 535 VDC for the push/pull output, 400 VDC for the phase splitter, regulated 120 VDC for the differential amplifier, and 6.3 VAC for the filaments (see **Figure 2**). Higher plate voltage could be used for the push/pull output circuit, resulting in greater peak output power. However, voltages above 600 VDC require special high-voltage wires, complicating the implementation of the design. In addition, the quiescent bias current of the tubes would have to be reduced, resulting in greater THD by pushing the bias points of the tubes further away from Class AB.

Each stage of the power supply is isolated to eliminate the power supply as a path of unintended feedback. The high-voltage output of T1 is rectified by V5, a 5U4GB. A pair

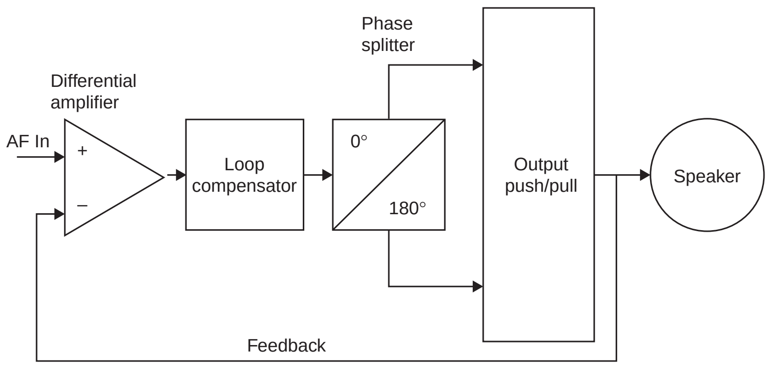

Figure 1: An amplifier block diagram

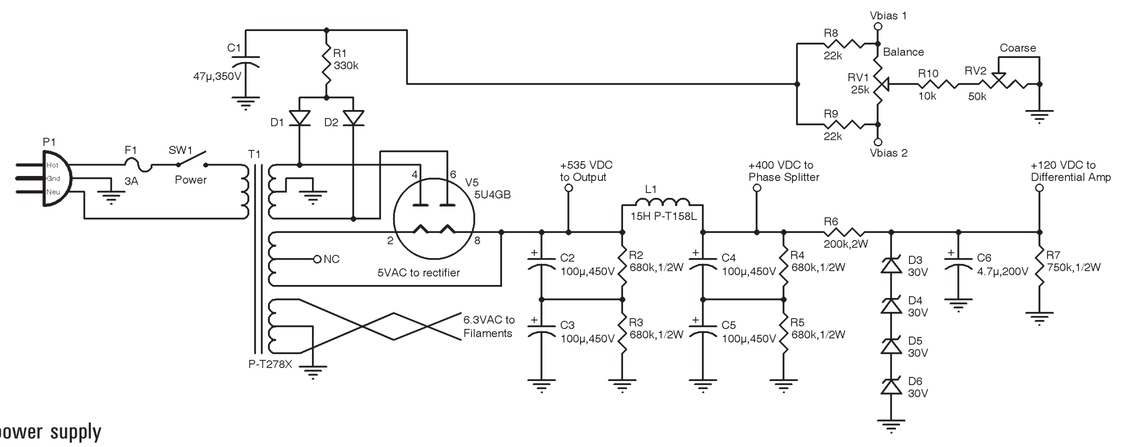

Figure 2: A power supply

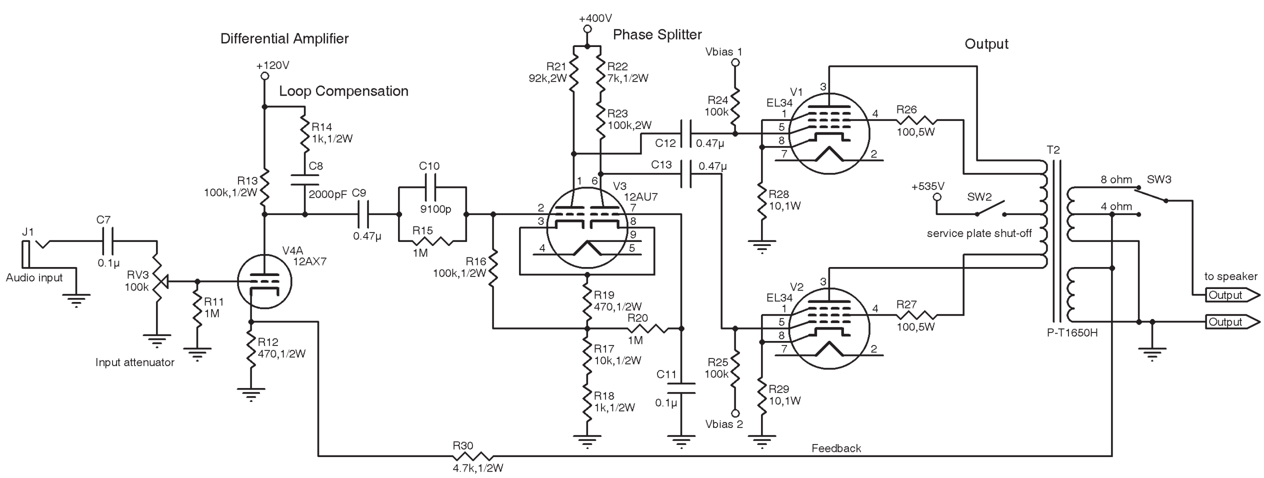

Figure 3: A complete amplifier

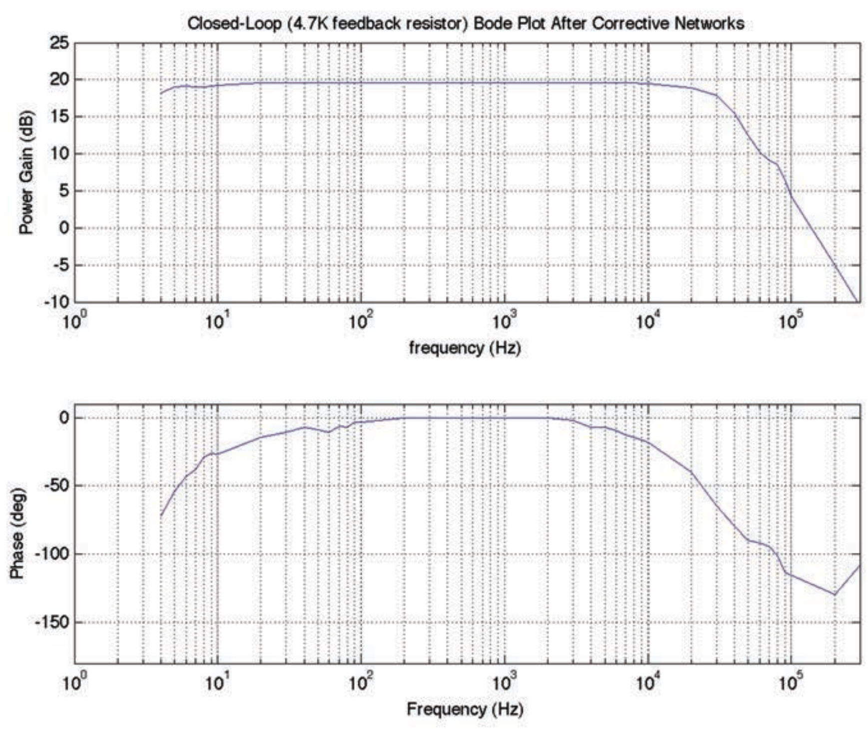

Figure 4: A mono-block power amplifier bode plot

Photo 2: A mono-block power amplifier

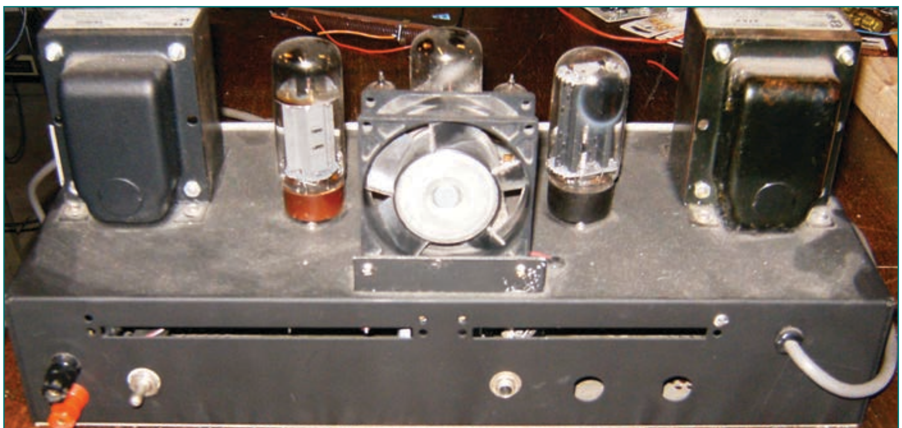

Photo 3: A rear view of the mono-block power amplifier

of 100-µF, 450-VDC capacitors (C2 and C3) filter the 535 VDC. A 15-H choke (L1) and two 100-µF, 450-VDC capacitors (C4 and C5) isolate the phase splitter from the output. A solid state 120-VDC Zener diode voltage regulator (D3–D6) isolates the differential amplifier from the phase splitter.

The output circuit uses a Hammond P-T1650H output transformer (T2) and a pair of EL34s in a push/pull configuration (V1 and V2 in **Figure 3**). A toggle switch on the secondary provides a convenient way to select speaker impedance. A toggle switch on the primary enables the plate voltage to be shut off during servicing. Direct grid bias is fed into the control grid g1 for both V1 and V2. Bias is set to approximately 37.5 mA through each tube by adjusting RV1 and RV2.

To initially set the bias, start by setting RV2 to a maximum value of 50 KΩ and RV1 to half of its value, 12.5 Ω. Then, slowly reduce RV2 while measuring the current through V1 and V2. As RV2 is increased, adjust RV1 so the same current is flowing through both tubes. Set the bias so both tubes are drawing 37.5 mA quiescent current. The bias should be periodically checked to compensate for tube aging.

This bias point is a compromise between suggested biasing for Class B (generally accepted 25–30 mA) and Class AB (60 mA) providing some reduction in crossover distortion compared to Class B.[3]

The phase splitter consists of a 12AU7 dual triode (V3), where V3a amplifies then outputs a phase-inverted waveform to g1 of V1. Similarly, V3b feeds its output to V2. However, V3b is coupled to the output of V3a through a common set of cathode resistors, producing a non-inverted output (see **Figure 3**).[4] Consequently, the two outputs from V3 are 180° out of phase. The magnitude of both outputs must be equalized by adding resistance in series with R23, where R22 was added to equalize the gain.

The audio input is fed in through J1 and through the potentiometer RV3 into the grid of a dual-triode

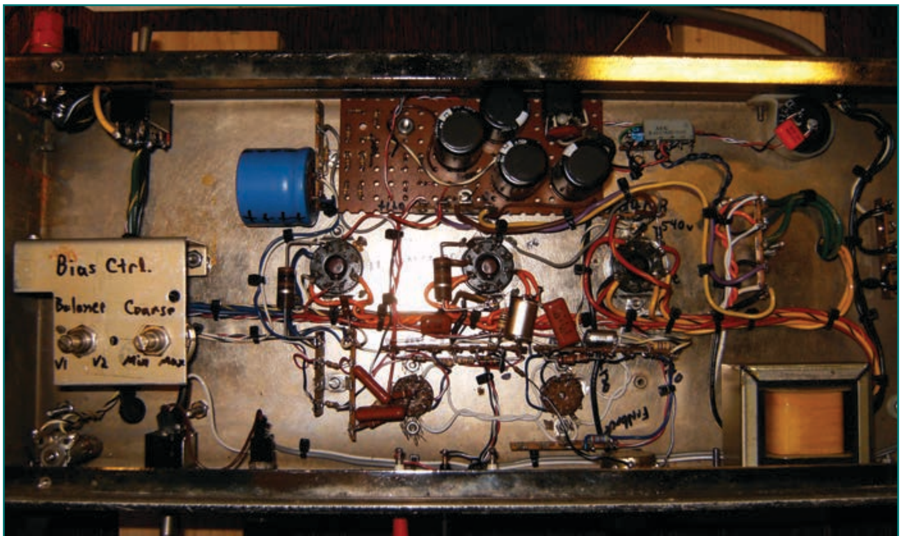

Photo 4: An inside, bottom view of the mono-block power amplifier

12AX7 (V4a). V4a amplifies the audio input and feeds it into the phase splitter while it simultaneously closes the negative feedback loop R30, which is in series with V4a's cathode and the secondary of T2. V4a is a differential amplifier, amplifying the difference between the input audio signal and the output of the amplifier.

The loop compensation circuit is part of the differential amplifier, which includes of R14, R15, C8, and C10. Prior to the installation of these components, the open-loop transfer function was measured by removing R30 and acquiring the bode plot from 4 Hz to 300 kHz. Results showed that the uncompensated amplifier crossed 180° of phase with significant open loop gain at both a low and a high frequency, resulting in oscillation at one or the other if the loop was closed. A compensation network was developed by using a method for both high- and low-frequency poles in tube feedback control systems.[5] The procedure is summarized in the *Radio Designer's Handbook*.[6] This loop compensator enables the amplifier to be unconditionally stable when the feedback loop is closed. Operating in a closed loop is desirable because it reduces THD, flattens the frequency response, and increases the effective bandwidth of the amplifier.

Photo 2, **Photo 3**, and **Photo 4** show the mono-block power amplifier. A bode plot of its closed-loop transfer function shows that it has excellent closed-loop bandwidth characteristics spanning 4 Hz to 30 kHz (see **Figure 4**). The maximum RMS output power was measured at 52 W. THD was measured at 0.675% at 1 kHz. These characteristics combined with the low-end cut-

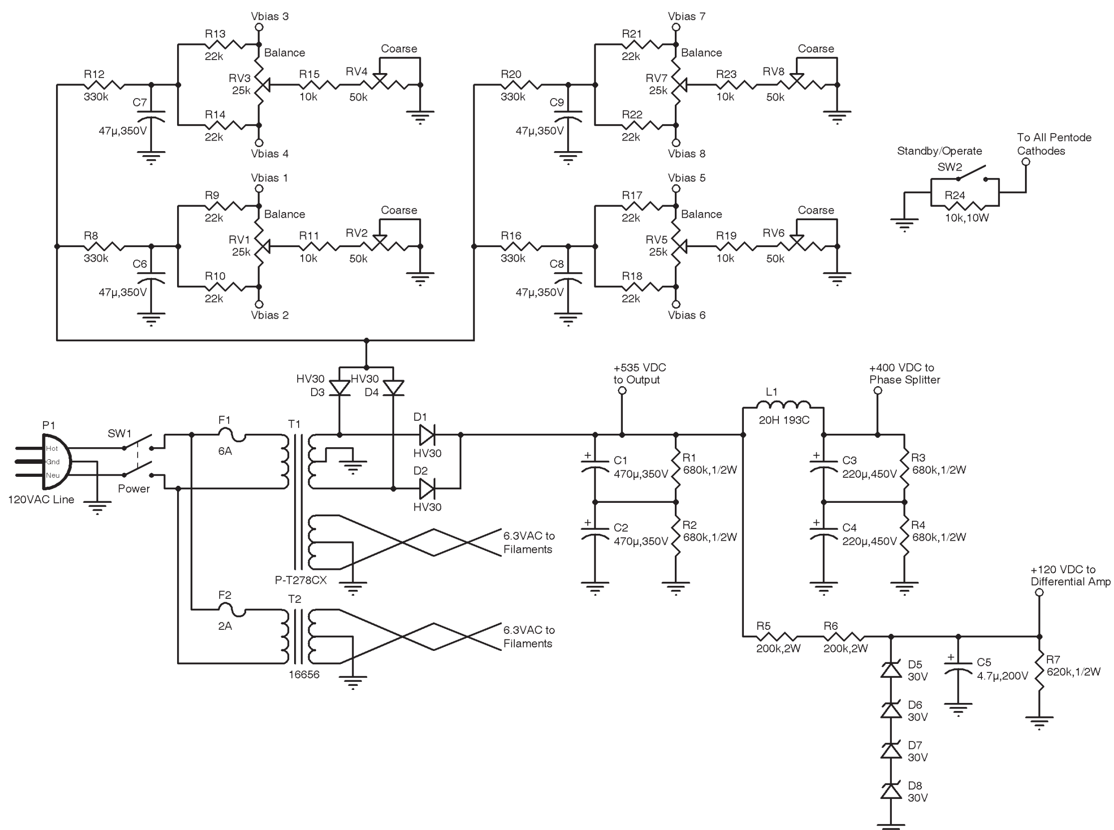

Figure 5: A quad-power amplifier power supply

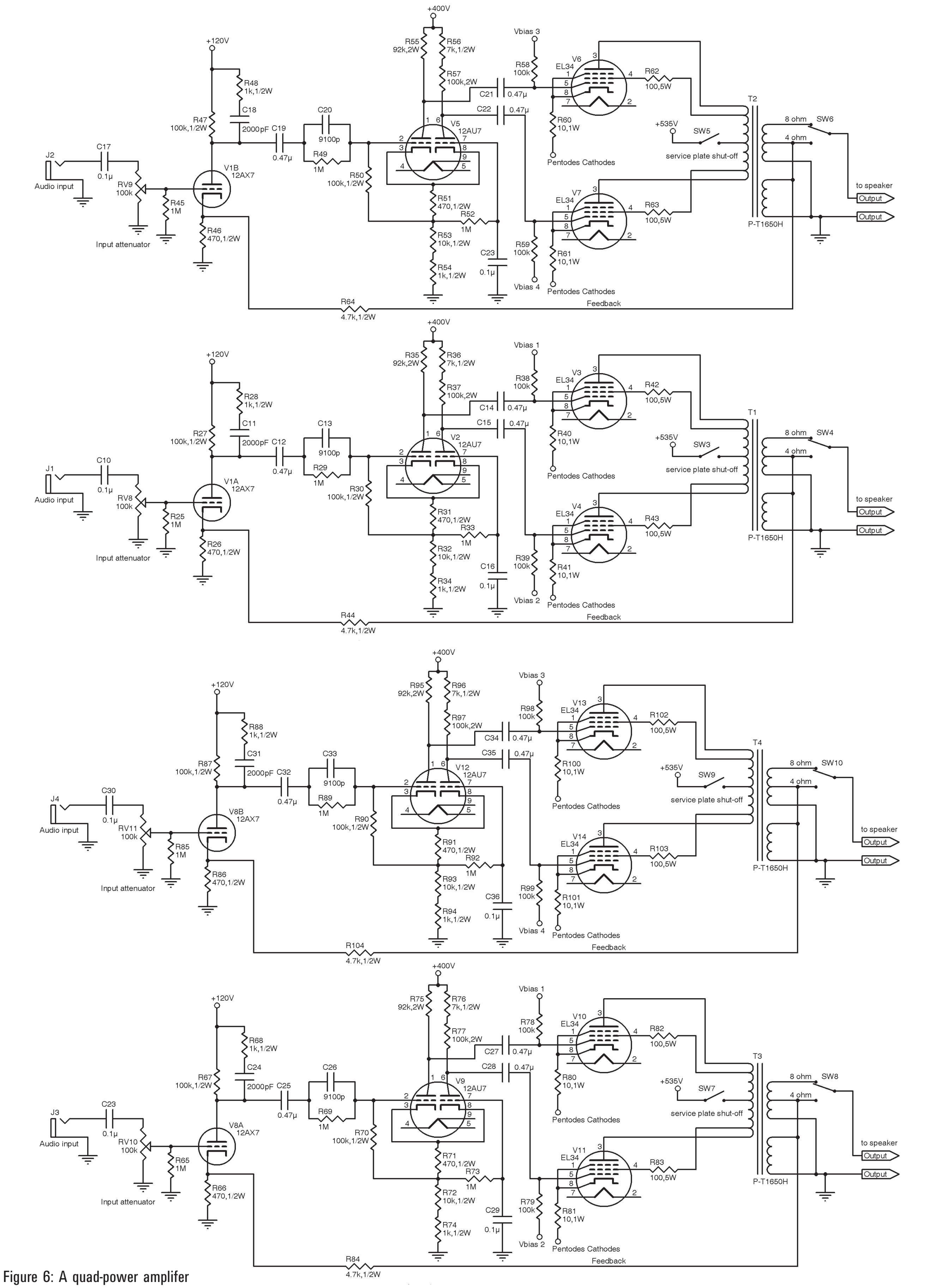

Figure 6: A quad-power amplifer

Photo 5: A mono-block power amplifier

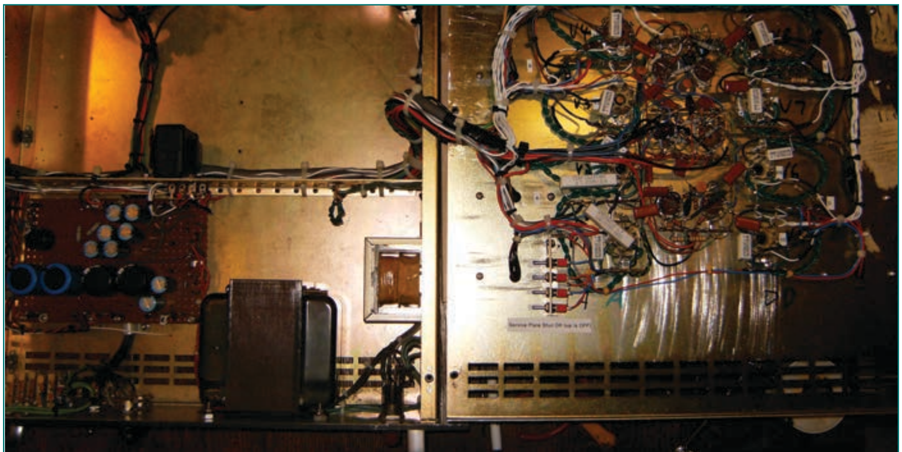

Photo 6: A rear view of the mono-block power amplifier

off frequency of 4 Hz shows that this amplifier is well suited for driving a subwoofer.

QUAD-POWER AMPLIFIER

The quad-power amplifier consists of four mono-block power amplifiers integrated into one chassis, using the same power supply. Diodes D1 and D2 were used for full-wave rectification (see **Figure 5**). For this reason a Standby/Operate switch, SW2, is connected between the cathodes of the EL34s and ground with a 10-Ω, 10-W resistor in parallel. This enables the cathodes of all pentodes to be lifted off ground during warm-up, protecting them against long-term cathode stripping. SW2 is left open for approximately 10–15 s while the tubes warm up then it is closed. A future design iteration might include the use of a vacuum tube rectifier in place of D1 and D2, which would eliminate the necessity for SW2.

The differential amplifiers, including 12AX7s (V1 and V8), are shared between two amplifiers while the rest

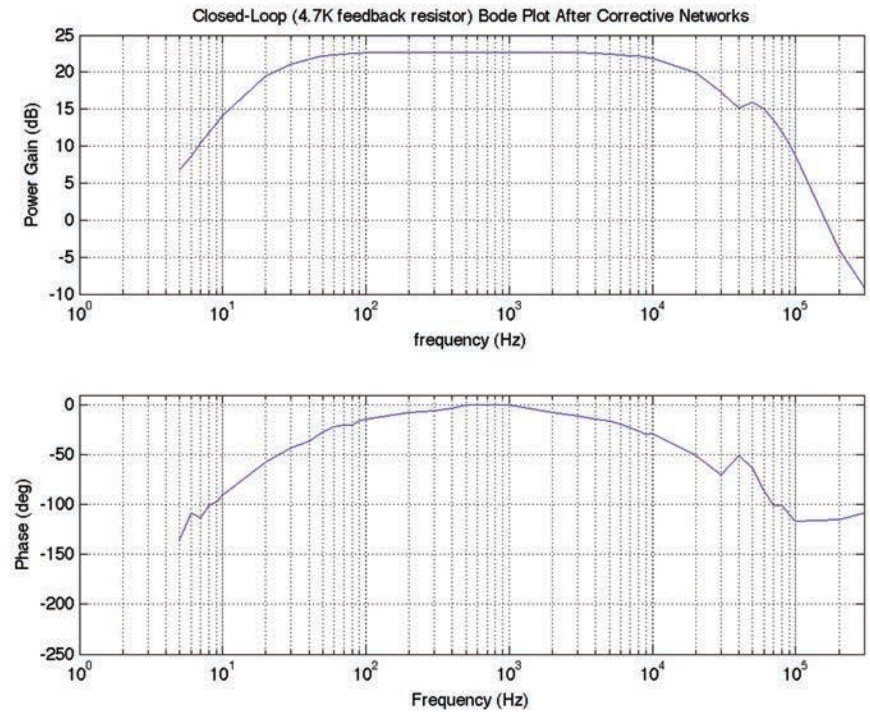

Figure 7: A bode plot of one amplifier inside of the quad power amplifier

of the amplifiers in the schematic are identical to the mono-block power amplifier (see **Figure 6**).

The quad-power amplifier is shown in **Photo 5** and **Photo 6**. The closed-loop bandwidth supports a full acoustical range of 22 Hz to 20 kHz (see **Figure 7)**. The output power was measured at 80-W RMS. Although the output pentodes are biased at 37.5 mA, the THD was measured at 0.45% at 1 kHz. These characteristics are excellent for powering the front and rear speakers of a home theater system.

HIT PLAY

I described the complete implementation of a vacuum-tube home theater using tubes throughout the analog signal chain. Special power amplifiers were developed that push the EL34 to the edge of their output power capability so loud action scenes can be experienced while producing less than 0.68% THD. Use this as a framework for your home theater audio project by either replicating these designs or substituting your components. It's time to build a monster home theater system. *aX*

REFERENCES

[1] L. Brown, *A Radar History of World War II Technical and Military Imperatives*, Institute of Physics Publishing, 1999.

[2] G. L. Charvat, "Vacuum Tube Home Theater System (Part 1): System Architecture," *audioXpress*, May 2012.

[3] Radio Corporation of America, *RCA Receiving Tube Manual*, Manual RC-30, 1975.

[4] K. O'Connor, *Principles of Power: A Practical Guide to Tube Power Amplifier Design*, Power Press Publishing, 1996.

[5] V. Learned, "Corrective networks for Feedback Circuits," Proc. I.R.E. 32.7, 1944.

[6] F. Langford-Smith, *Radio Designer's Handbook*, 4th Edition, Reed Educational and Professional Publishing Ltd., 1997.

[7] B. Rozenblit, *Beginner's Guide to Tube Audio Design*, Audio Amateur Press, 1997.

 By Vance Dickason (United States)

Another Look at Scan-Speak's 12MU/473100

A compact high-end home audio driver put to the test

Photo 1: The Scan-Speak 12MU/4731T00

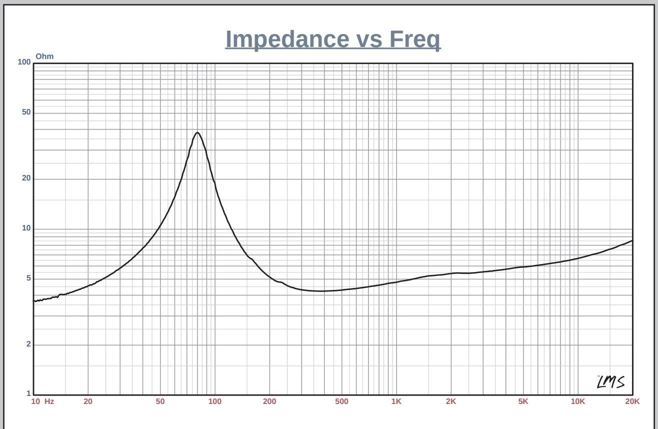

Figure 1: The Scan-Speak 12MU/4731T00 free-air impedance plot

I had begun testing the Scan-Speak 12MU/4731T00 (see **Photo 1**), when I recalled that this driver had been previously tested. Looking through the *Voice Coil* archives, I found that I had characterized the Scan 12MU in the July 2009 issue. Rather than put this back on the shelf, I thought readers might find it interesting to not only take another look at this good-sounding high-end midrange again, but also to compare current production with the data taken nearly two years ago. Knowing the emphasis on quality and quality control that Scan puts into its production, I expected the data to turn out very close, which indeed it did.

As part of Scan-Speak's Illuminator series of the drivers, the 12MU is built on the same great looking frame as the other Illuminator woofers, with the same, but scaled down, underhung (gap height is 13 mm, with a 6-mm voice coil height) neodymium ring magnet motor structure (see **Photo 2**). Like the woofer motor, the front plate is shaped to "guide" the backside airflow around the motor. In terms of features, the 12MU uses a single layer uncoated curvilinear embossed paper cone as opposed to the two-layer embossed cone used for the 15WU and 18WU woofers. I assume that the embossing on the 12MU cone is more cosmetic than functional and is intended to match the "look" of the Illuminator woofers. The uncoated paper dust cap is also embossed to complete the cosmetic appearance of the 12MU. Other features include a flat-cloth spider, a coated-foam surround (Mmd for this driver is only 5.2), a copper shorting ring, and lead wires that are terminated to gold-plated terminals.

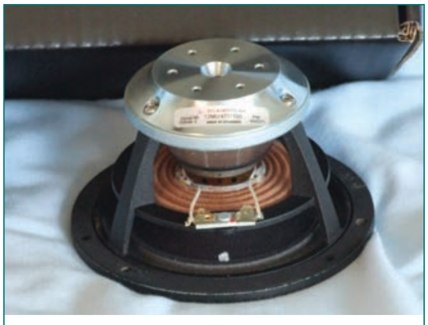

Photo 2: The 12MU is built with a neodymium ring magnet motor structure.

Testing commenced with the driver clamped to a rigid test fixture in free air, with voltage and current sweeps taken at 0.3 V, 1 V, 3 V, 6 V, and 10 V. The 10-V test proved to be somewhat nonlinear and was not used, but it was close, which is amazing for a 4" driver. The remaining eight 550-point stepped sine wave sweeps for each 12MU midrange sample were post-processed. The voltage curves were divided by the current curves (admittance) to create impedance curves, phase was added using LMS calculation method, and along with the accompanying voltage curves, saved to the LEAP 5 Enclosure Shop software. In addition to the LEAP 5 LTD model results, I also created a LEAP 4 TSL model set of parameters using just the 1-V free-air curves. The final data set, which includes the multiple voltage impedance curves for the LTD model and the 1-V impedance curve for the TSL model were selected and the parameters created in order to perform the computer box simulations (see **Figure 1** for the 1-V free-air impedance curve). **Table 1** compares the LEAP 5 LTD and TSL data and factory parameters for both of the Scan-Speak 4" samples measured for this issue. **Table 2** provides the data for the pair measured in July 2009.

As I expected, the Scan data was very consistent from 2009 and 2012, with about the same variation between LEAP parameter calculation results for the Scan 12MU midrange and the factory data. As before, the Fs/Qt ratios are reasonably close to the Scan-Speak factory data. Given this, I set up computer enclosure simulations using the LEAP LTD parameters for Sample 1, the same sealed box volumes used in the July 2009 report. For the first closed box simulation I used a 38-ci enclosure with 50% fiberglass fill material. For the second sealed box, I used a larger volume of 62ci Qb3 also with 50% fiberglass fill material.

Figure 2 displays the results for the 12MU/4731T00 in the two sealed boxes at 2.83 V and at a voltage level sufficiently high enough to increase cone excursion to Xmax + 15% (4 mm for the 12MU). This resulted in a F3 = 181 Hz with a box/driver Qtc of 0.67 for the 38-ci design and a –3 dB = 156 Hz with a Qtc = 0.57 for the 62-ci simulation. The July 2009 results were close to the same F3/Qtc with a F3 = 171 Hz with a box/driver Qtc of 0.7 for the 38-ci design and a –3 dB = 150 Hz with a Qtc = 0.6 for the 62-ci simulation.

Increasing the voltage input to the simulations until the maximum linear cone excursion was reached generated 110 dB

	TSL model		LTD model		Factory
	sample 1	sample 2	sample 1	sample 2	
Fs	79.4 Hz	66.2 Hz	74.5 Hz	62.5 Hz	64 Hz
Revc	3.11	3.03	3.11	3.03	3.1
Sd	0.0057	0.0057	0.0057	0.0057	0.0058
Qms	4.18	3.87	3.48	3.32	3.64
Qes	0.37	0.30	0.30	0.27	0.26
Qts	0.34	0.28	0.28	0.25	0.24
Vas	3.4 ltr	4.9 ltr	3.9 ltr	5.6 ltr	5.4 ltr
SPL 2.83 V	88.5 dB	88.6 dB	89.0 dB	88.9 dB	90 dB
Xmax	3.5 mm	3.5 mm	3.5 mm	3.5 mm	3.5 mm

Table 1: Scan-Speak 12MU/4731T00 midrange, tested March 2012

	TSL model		LTD model		Factory
	sample 1	sample 2	sample 1	sample 2	
Fs	75.3 Hz	76.5 Hz	73.2 Hz	74.7 Hz	64 Hz
Revc	3.04	2.91	3.04	2.91	3.1
Sd	0.0057	0.0057	0.0057	0.0057	0.0058
Qms	3.58	3.98	3.13	3.53	3.64
Qes	0.34	0.31	0.30	0.30	0.26
Qts	0.31	0.31	0.27	0.27	0.24
Vas	3.6 ltr	3.4 ltr	3.8 ltr	3.7 ltr	5.4 ltr
SPL 2.83 V	88.4 dB	88.6 dB	88.7 dB	88.9 dB	90 dB
Xmax	3.5 mm	3.5 mm	3.5 mm	3.5 mm	3.5 mm

Table 2: Scan-Speak 12MU/4731T00 midrange, tested July 2009

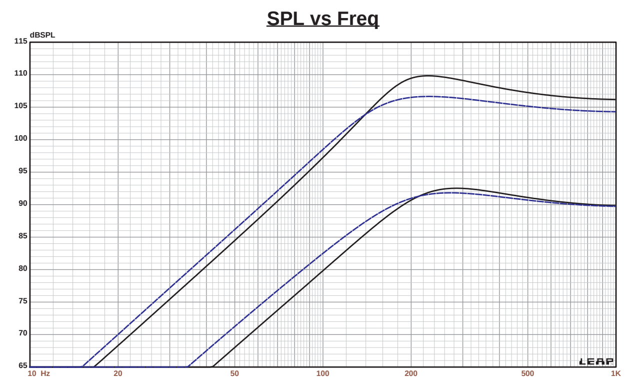

Figure 2: Scan-Speak 12MU/4731T00 computer box simulations (black solid = sealed 1 @ 2.83 V; blue dash = sealed 2 @ 2.83 V; black solid = sealed 1 @25 V; blue dash = sealed 2 @18 V

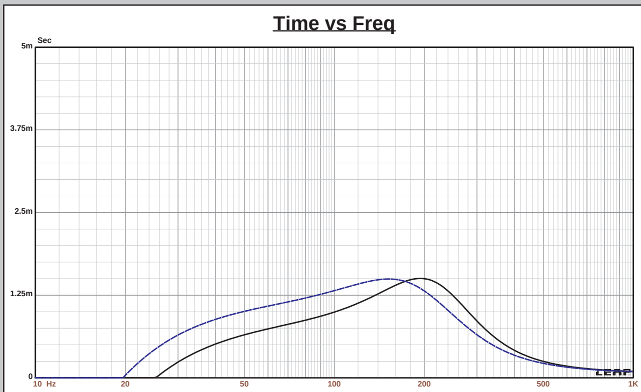

Figure 3: Group delay curves for the 2.83-V curves in Figure 2

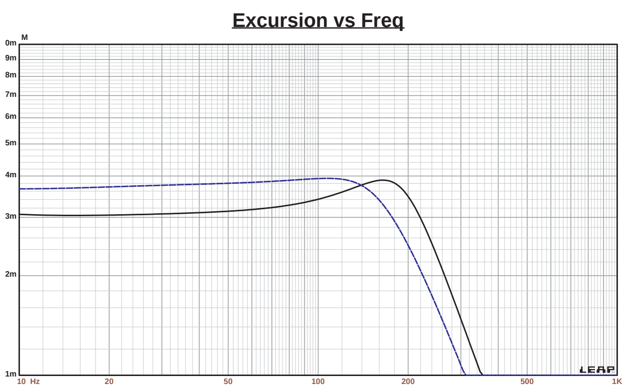

Figure 4: Cone excursion curves for the 25/18-V curves in Figure 2

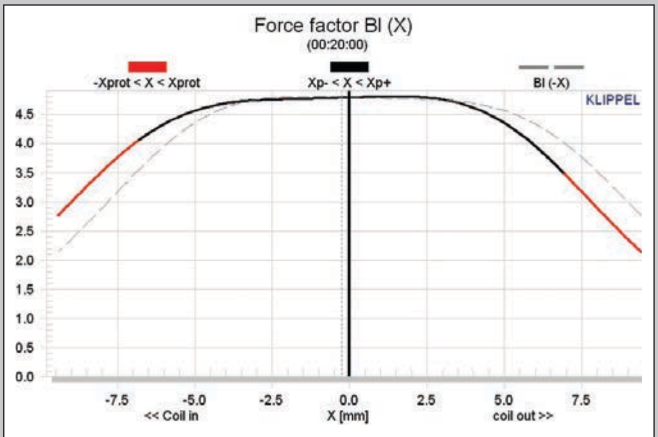

Figure 5: Klippel Analyzer Bl (X) curve for the Scan-Speak 12MU/4731T00

at 25 V for the sealed-enclosure simulation and 106 dB with an 18-V input level for the larger closed box (see **Figure 3** and **Figure 4** for the 2.83-V group delay curves and the 25/19-V excursion curves). Obviously, the 12MU, as with any midrange, will be used in conjunction with a band-pass filter network, but this information can help locate an appropriate crossover frequency. It is often difficult to locate the high-pass section of a band-pass filter within one octave or less of the resonance of a midrange device and it sometimes requires an LCR conjugate circuit to prevent the circuit interaction.

Klippel analysis for the Scan 12MU midrange produced the Bl(X), Kms(X), and Bl and Kms symmetry range plots given in **Figures 5–8**. The Bl(X) curve for the 12MU (see

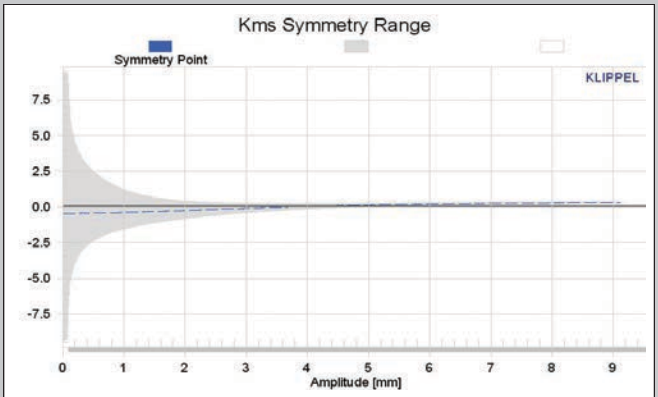

Figure 6: Klippel Analyzer Bl symmetry range curve for the Scan-Speak 12MU/4731T00

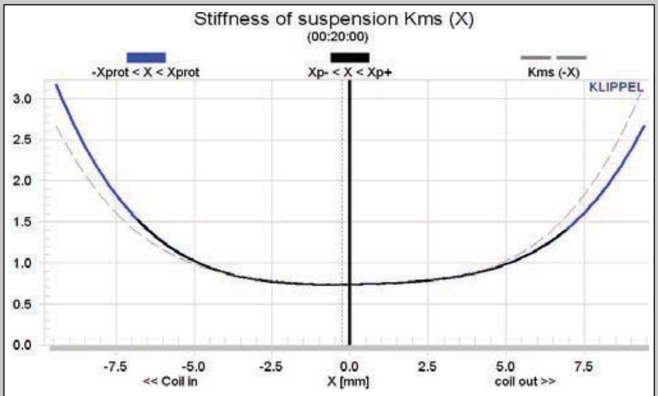

Figure 7: Klippel Analyzer mechanical stiffness of suspension Kms (X) curve for the Scan-Speak 12MU/4731T00

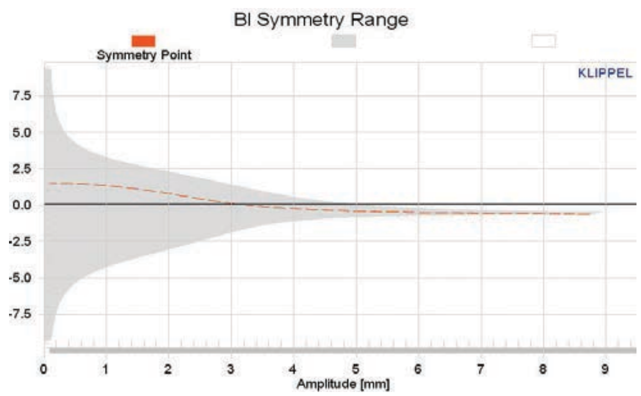

Figure 8: Klippel Analyzer symmetry range curve for the Scan-Speak 12MU/4731T00

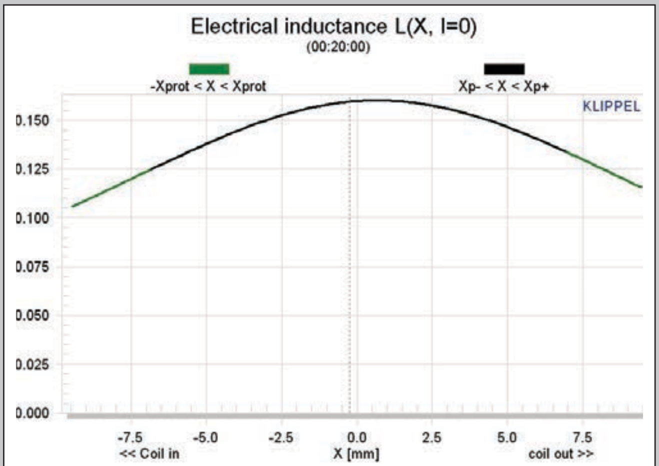

Figure 9: Klippel Analyzer Le (X) curve for the Scan-Speak 12MU/4731T00

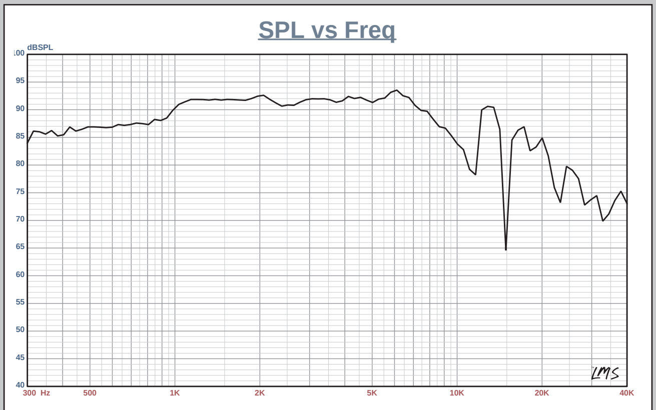

Figure 10: Scan-Speak 12MU/4731T00 on-axis frequency response

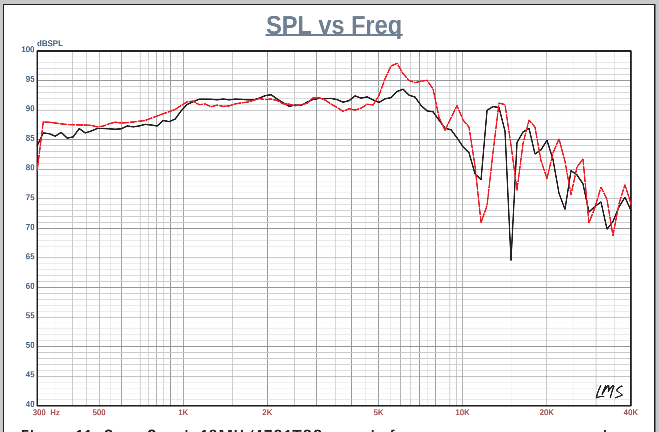

Figure 11: Scan-Speak 12MU/4731T00 on-axis frequency response comparison of the February 2012 sample to the July 2009 sample

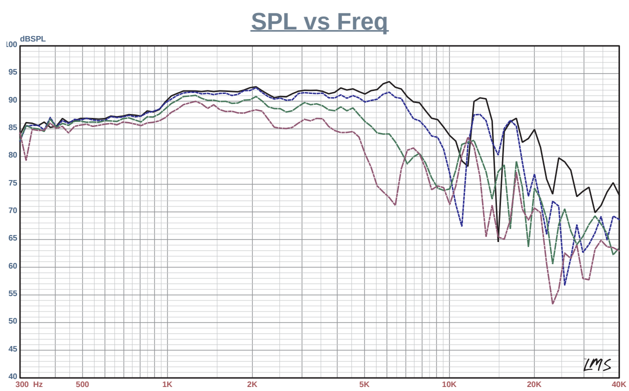

Figure 12: Scan-Speak 12MU/4731T00 on- and off- frequency response

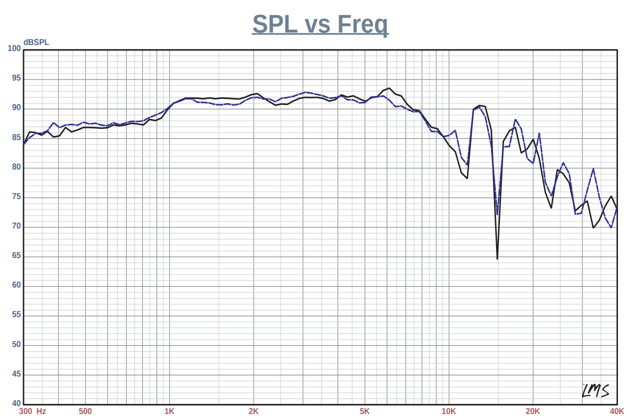

Figure 13: Scan-Speak 12MU/4731T00 two-sample comparison

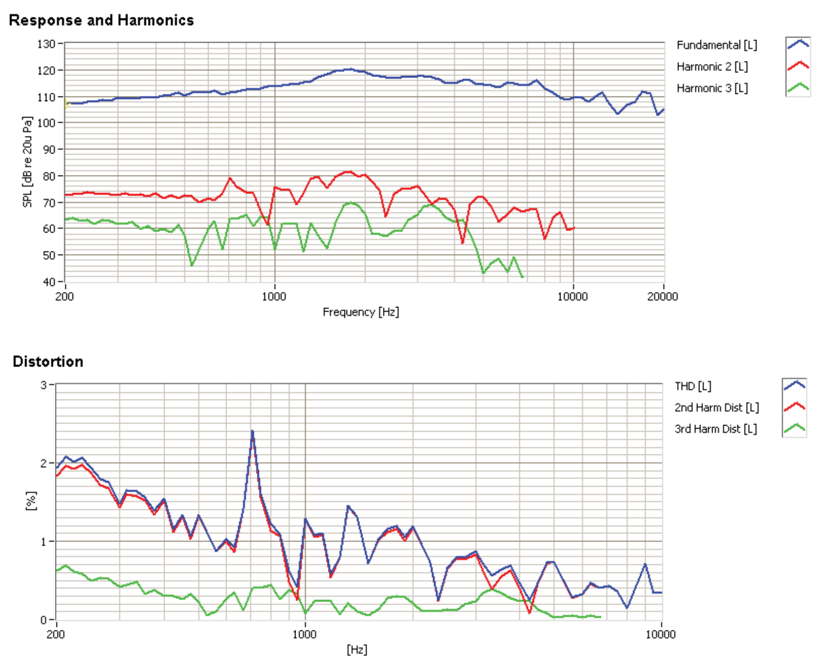

Figure 14: Scan-Speak 12MU/4731T00 SoundCheck distortion plot

Figure 5) is moderately broad and very symmetrical, which is more like a woofer than a midrange. Looking at the Bl symmetry range curve in **Figure 6**, there is a 0.5-mm rearward (coil-in) offset that goes to 0 mm at the physical Xmax position (3.5 mm for the 12MU). **Figure 7** and **Figure 8** show the Kms(X) and Kms symmetry range curves for the12MU. The Kms(X) curve also is very symmetrical. However, since the application is as a midrange that will always have a band-pass filter, excursion will be limited, regardless of how good the Klippel data for this driver looks. Even considering this, the forward coil-out offset at rest is only 1.5 mm resolving to 0 mm at about 3 mm of travel. Displacement-limiting numbers calculated by the Klippel analyzer for the Scan midrange were 6.1 mm (i.e., XBl @ 82% Bl) and for XC @ 75% Cms minimum was 4.8 mm, which means that for this 4" midrange, the compliance is the most limiting factor for prescribed distortion level of 10%. Regardless, it is still significant that both XBl and XC numbers occur beyond the physical Xmax. The 12MU may be offered as a midrange, but it's really not so bad as a woofer! **Figure 9** shows the inductance curves Le(X) for the 12MU/4731T00, which shows a very small 0.15-mH inductance change across the operating range, again due to the copper shorting ring and overall motor construction.

With the Klippel testing finalized, I mounted the 12MU driver in an enclosure that had a 15" × 5" baffle filled with foam damping material and proceeded to measure the driver frequency response both on- and off-axis from 300 Hz to 40 kHz at 2.83 V/1 m using a 100-point gated sine wave sweep. **Figure 10** shows the 12MU's on-axis response displaying a smooth rising response to about 1 kHz, flattening out above that frequency. **Figure 11** compares the April 2012 on-axis curve to the July 2009 version. These two curves are very close, but if anything, Scan has improved the response by eliminating the 5.3-Hz peak that was in the previous test.

Figure 12 shows the on- and off-axis frequency response at 0°, 15°, 30°, and 45°. The –3 dB at 30°, with respect to the on-axis curve, occurs at 4 kHz, so a 4-to-5-kHz crossover frequency would be appropriate for this driver. And finally, **Figure 13** shows the two-sample SPL comparisons for the 4" Scan-Speak midrange driver, showing a good match within 1 dB or less throughout the operating range.

For the last body of testing on the Scan-Speak 12MU midrange, I used the Listen, Inc. SoundCheck analyzer (courtesy of Listen, Inc.) and the SCM microphone and power supply to measure distortion and generate time-frequency plots. To set up the distortion measurement, I mounted the woofer rigidly in free air, and set the SPL to 94 dB at 1 m (4.8 V), using a noise stimulus (SoundCheck has a software generator and SPL meter as

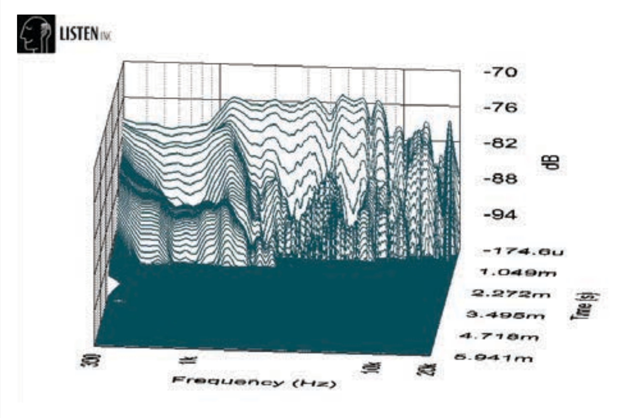

Figure 15: Scan-Speak 12MU/4731T00 SoundCheck CSD waterfall plot

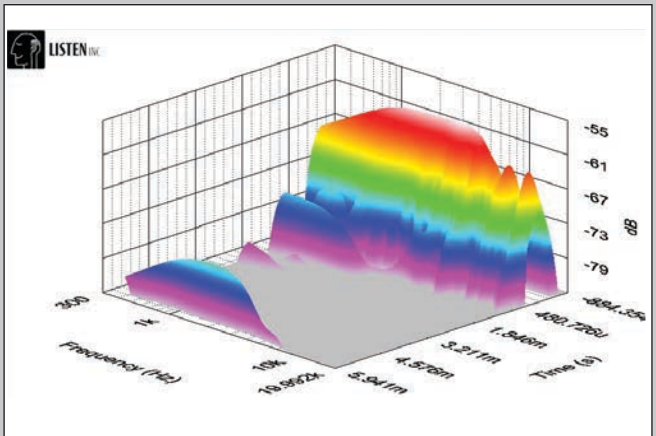

Figure 16: Scan-Speak 12MU/4731T00 SoundCheck Wigner-Ville plot

two of its utilities). Then, I measured the distortion with the SCM microphone placed 10 cm from the phase plug. This produced the distortion curves shown in **Figure 14**.

For the last test on the Scan 12MU, I used the SoundCheck analyzer to get a 2.83 V/1-m impulse response for this driver and imported the data into Listen, Inc.'s SoundMap time/frequency software. The resulting CSD waterfall plot is shown in **Figure 15** and the Wigner-Ville (for its better low-frequency performance) plot is shown in **Figure 16**.

What attracts high-end loudspeaker manufacturers to Scan-Speak products is not only their musical sound quality, but the overall precision and consistency that goes along with Scan's manufacturing culture. It was fun to examine this driver, compare it with data I took nearly two years ago, and end up with the results I expected.

For more information, visit the Scan-Speak website at www.scan-speak.dk. *aX*